Centromeric CENP-A loading requires accurate mitotic timing, which is linked to checkpoint proteins

Anne Laure Pauleau[1,2,3], Andrea Bergner[1,2,3,4], Janko Kajtez[1,5], and Sylvia Erhardt[1,2,3]

[1] Center for Molecular Biology of Heidelberg University (ZMBH), Im Neuenheimer Feld 282, 69120 Heidelberg, Germany.

[2] DKFZ-ZMBH-Alliance, 69120 Heidelberg, Germany.

[3] CellNetworks Excellence Cluster, Heidelberg University, 69120 Heidelberg, Germany.

[4] current address: Max Planck Institute for Medical Research, Heidelberg, 69120, Germany

[5] current address: Department of Micro- and Nanotechnology, Technical University of Denmark, Produktionstorvet 423, DK-2800 Kgs. Lyngby, Denmark.

Correspondence to Sylvia Erhardt: s.erhardt@zmbh.uni-heidelberg.de

Abstract

A defining feature of centromeres is the presence of the histone H3 variant CENP-A that replaces H3 in a subset of centromeric nucleosomes. In *Drosophila* cultured cells CENP-A deposition at centromeres takes place during the metaphase stage of the cell cycle and strictly depends on the presence of its specific chaperone CAL1. How CENP-A loading is restricted to mitosis is unknown. We found that overexpression of CAL1 is associated with increased CENP-A levels at centromeres and completely uncouples CENP-A loading from mitosis. Moreover, CENP-A levels inversely correlate with mitosis duration. We found that CAL1 interacts with the spindle assembly checkpoint protein and RZZ complex component Zw10 and thus constitutes the anchor for the recruitment of RZZ. Therefore, CAL1 controls CENP-A incorporation at centromeres both quantitatively and temporally, connecting it to the spindle assembly checkpoint to ensure mitotic fidelity.

30 **Introduction**

31 The formation of two genetically identical daughter cells with a correct and stable genome is
32 of utmost importance during mitosis. Condensed chromosomes are attached and segregated
33 to the opposing poles of the dividing cell at anaphase by the mitotic spindle. At the interface
34 between the chromosomes and the spindle microtubules lies the kinetochore. This multi-
35 protein complex is formed by the components of the KMN network (formed by the Knl1
36 complex, the Mis12 complex and the Ndc80 complex) (1). The Ndc80 complex is mainly
37 responsible for connecting microtubules with kinetochores while the Knl1 complex primarily
38 functions to coordinate the Spindle Assembly Checkpoint (SAC) (2). The SAC delays entry into
39 anaphase until all chromosomes are properly attached and aligned at the metaphase plate.
40 The metaphase to anaphase transition is controlled by the activation by Cdc20 of the APC/C,
41 a multisubunit ubiquitin ligase that triggers the degradation of cell cycle regulators by the
42 proteasome (3). The SAC proteins Mad2, BubR1, and Bub3 sequester Cdc20 forming the
43 Mitotic Checkpoint Complex (MCC) thereby preventing the activation of the APC/C. In
44 addition, other proteins have been implicated in SAC activity including Bub1, Mad1, the Mps1
45 and Aurora B kinases and the RZZ complex (formed by the three proteins Rough Deal (ROD),
46 Zw10 and Zwilch) (4). Finally, the Mis12 complex serves as a hub interacting with all
47 kinetochore complexes as well as with the centromere (2).

48 The kinetochore assembles on centromere during mitosis, a highly specialized chromatin
49 region that is defined by an enrichment of nucleosomes containing the histone H3 variant
50 CENP-A, also called CID in *Drosophila*. In contrast to canonical histones, CENP-A deposition at
51 centromeres is independent of DNA replication and is temporally restricted to a specific cell
52 cycle stage, which varies between organisms: late telophase/early G1 in mammalian cultured
53 cells (5), G2 in S. pombe and plants (6-8), and mitosis to G1 in *Drosophila* (9-12). CENP-A

54 loading requires the action of licensing factors such as the Mis18 complex that modify
55 centromeric chromatin (13), as well as of its dedicated chaperone: HJURP in humans, Scm3 in
56 fungi and CAL1 in *Drosophila* (14-20). Any deregulation of CENP-A and its loading machinery
57 results in the misincorporation of CENP-A into chromosome arm regions. Misincorporated
58 CENP-A is rapidly degraded (21-23). If, however, CENP-A-containing nucleosomes remain at
59 non-centromeric sites ectopic formation of functional kinetochores can occur that may lead
60 to chromosomes segregation defects and aneuploidy (24-26).
61 The timing of CENP-A is particularly intriguing in *Drosophila* cultured cells as centromeric
62 CENP-A is replenished during prometaphase-metaphase thus coinciding with kinetochore
63 assembly. In *Drosophila melanogaster,* two other proteins are constitutively present at
64 centromeres and essential for centromere function: the conserved protein CENP-C (27) and
65 CENP-A chaperone CAL1. CENP-C has been shown to act as a linker between CENP-A
66 nucleosomes and the Mis12 complex therefore providing a platform for kinetochore assembly
67 (28). CENP-C is also implicated in CENP-A replenishment at centromeres during mitosis by
68 recruiting CAL1 (18, 20). CAL1 interacts with CENP-A in both pre-nucleosomal and
69 nucleosomal complexes (18) and is necessary for CENP-A protein stabilization via Roadkill-
70 Cullin3-mediated mono-ubiquitination (29). Moreover, CAL1 has been previously shown to
71 be the limiting factor for CENP-A centromeric incorporation in fly embryos (30). However,
72 differences in centromere assembly have been reported between *drosophila* cultured cells
73 and tissues. Firstly, CENP-A loading has been shown to take place during mitotic exit in early
74 embryos (9) and during prometaphase to early G1 in cultured cells (10, 12). Second, CENP-C
75 incorporates concomitantly to CENP-A in embryos (9) while this time window seems to be
76 larger in cultured cells (10). We therefore set out to determine more precisely the function of
77 CAL1 in CENP-A loading regulation in *drosophila* cultured cells.

78 During the course of these studies we found that overexpression of CAL1 not only increases
79 CENP-A abundance at centromeres, it also uncouples CENP-A loading from mitosis. Strikingly,
80 we discovered a co-dependence of mitotic duration and accurate CENP-A loading that is likely
81 mediated by the interaction of the loading machinery of CENP-A with the Spindle Assembly
82 Checkpoint component Zw10. These data suggest an intricate coordination of the spindle
83 assembly checkpoint, CENP-A loading, and mitotic duration.
84
85 **Results**
86 **CAL1 levels regulate the amount of CENP-A at centromere.**
87 In order to understand whether levels of CAL1 influence CENP-A loading, we overexpressed
88 CAL1 in S2 cells from a copper-inducible pMT promoter. Induced CAL1 localized to
89 centromeres and the nucleolus in a majority of transfected cells (84 %), similar to endogenous
90 CAL1. Cytoplasmic and/or nucleoplasmic CAL1 were visible in about 16 % of the cells (Fig. 1A).
91 Augmented total CAL1 protein levels (2-fold increase; Fig. 1B) led to increased CAL1 levels at
92 centromeres (Fig. 1C) and caused an increase of both endogenous and overexpressed CENP-
93 A (GFP and SNAP) levels (Fig. 1D). Importantly, however, CENP-A was localizing to
94 centromeres only and we did not detect CENP-A at any other chromatin regions on
95 metaphase chromosomes (Fig. 1E-F). This result indicates that CAL1 overexpression does not
96 lead to misincorporation of CENP-A to non-centromeric sites. In contrast to previous
97 observations in embryos (30), centromeric CENP-A levels were increased by up to 2 fold after
98 24 hours of CAL1 overexpression (Fig. 1G). Surprisingly, CENP-C levels remained largely
99 unaffected by CAL1 overexpression (Fig. 1F-G). These results show that the abundance of
100 CENP-A at centromeres is regulated by the available amount of CAL1.
101

102 To test whether the increased CENP-A level is caused by increased CENP-A loading we used
103 the SNAP-tag technology in a quench-chase-pulse experiment to label newly synthesized and
104 incorporated CENP-A (5). At day 1 of CAL1 induction, we quenched existing SNAP-CENP-A
105 molecules with a non-fluorescent ligand, cultured the cells for 24 hours to allow
106 approximately one additional cell division, then marked newly synthesized SNAP-CENP-A
107 molecules with a fluorophore and measured fluorescent intensity of newly incorporated
108 SNAP-CENP-A at centromeres (Fig. 1H). Similar to what we observed for GFP-CENP-A,
109 significantly more SNAP-CENP-A incorporated into centromeres in CAL1 overexpressing cells
110 (Fig. 1H-I). These data confirm that CENP-A centromeric levels are regulated by CAL1 and that
111 CAL1 overexpression specifically increases incorporation of newly synthesized CENP-A at
112 centromeric chromatin.
113
114 **Overexpression of CAL1 leads to centromeric CENP-A loading outside of mitosis.**
115 CENP-A loading takes place during prometaphase-metaphase in *Drosophila* S2 cells (10). To
116 determine if CAL1 overexpression changes CENP-A loading pattern during mitosis, we
117 measured Fluorescence Recovery After Photobleaching (FRAP) of CENP-A, on the assumption
118 that fast recovery of the signal at centromeres corresponds to active loading of CENP-A. We
119 partially bleached GFP-CENP-A signal during prophase and followed recovery of the signal at
120 centromeres until anaphase. We observed a partial recovery of GFP-CENP-A at centromeres
121 in control cells, confirming previous reports that loading of new CENP-A takes place during
122 mitosis (10) (Fig. 2A-B). Surprisingly, GFP-CENP-A recovery rate decreased in CAL1-
123 overexpressing cells compared to control cells (Fig. 2B). One possible explanation for this
124 observation could be that CENP-A centromeric levels get replenished at a different time point
125 in CAL1-overexpressing cells. Indeed, besides loading in mitosis, CENP-A loading has also been

126 reported in G1 in S2 cells (12). We therefore followed cells through mitosis, partially bleached
127 GFP-CENP-A in early G1 and measured GFP-CENP-A signal intensity for 3 hours. However, we
128 did not detect any recovery of the bleached GFP-CENP-A signal (Fig. S1A). We explained these
129 results by the likely absence of any measurable GFP-CENP-A loading in early G1.
130
131 Since the availability of CAL1 seems to be the crucial determinant for CENP-A incorporation,
132 we tested if CAL1-overexpressing cells incorporate CENP-A into centromeric chromatin
133 outside mitosis. Thus, we arrested cells at the metaphase to anaphase transition using the
134 proteasome inhibitor MG132 treatment for 2 hours, blocked existing SNAP-CENP-A molecules
135 using SNAP-Block and cultured the cells for an additional 4 hours in the presence of MG132
136 (Fig. S1B) similar to a previously published protocol (10). Whereas 10 % of uninduced pMT-
137 CAL1 cells loaded SNAP-CENP-A, the induction of pMT-CAL1 and resulting overexpression of
138 CAL1 led to an incorporation of newly synthesized SNAP-CENP-A in about 40 % of the cells,
139 pointing to loading outside of mitosis (Fig. S1B). To confirm that overexpressed CAL1 indeed
140 loads CENP-A to centromeres outside of mitosis, we followed newly synthesized SNAP-CENP-
141 A live by time-lapse microscopy. We blocked existing SNAP-CENP-A with SNAP-Block, washed
142 and added SNAP-640 fluorophore (31) to the culture medium in order to stain newly
143 synthesized SNAP-CENP-A molecules. Despite some aggregation of the dye, SNAP-CENP-A
144 loading at centromeres was discernable in both CAL1 overexpressing and control cells (Fig.
145 2C). We only analyzed cycling cells that eventually entered mitosis during the course of
146 imaging and determined whether and when they incorporated SNAP-CENP-A. We found that
147 38 % of uninduced control cells had SNAP-CENP-A signals at centromeres by the end of the
148 imaging (Fig. 2C-E; video 1). Of those, 91 % loaded SNAP-CENP-A during mitosis and 9 % just
149 after the cell exited mitosis. In contrast, 81 % of cycling CAL1-overexpressing cells had SNAP-

150 CENP-A signals at centromeres (Fig. 2C-E; video 2), and of those 31 % loaded before mitosis
151 and 51 % after the cells exited mitosis. The specificity of the signal was verified by co-staining
152 with anti-CENP-A antibody immediately after block (0 min), and 20 hours of incubation with
153 SNAP-640 (Fig. S1C). No SNAP-CENP-A was detected directly after SNAP-block treatment,
154 confirming the efficient quenching of old SNAP-CENP-A molecules (Fig. S1C). After 20 hours
155 newly synthesized SNAP-CENP-A perfectly co-localized with total CENP-A signals at
156 centromeres. Interestingly, when we counted the percentage of cells that displayed SNAP-
157 CENP-A at centromeres in these fixed samples we did not observe any differences between
158 control and CAL1-overexpressing cells after 20 h (Fig. S1D). However, SNAP-CENP-A
159 centromeric intensity was four times higher in CAL1-overexpressing cells than in control cells
160 (Fig. S1E). This suggests that low SNAP-CENP-A protein levels were masked in the presence of
161 excess SNAP dye in live cell analysis. Nevertheless, the analysis of SNAP-CENP-A loading in
162 cycling cells revealed that cells overexpressing CAL1 load CENP-A throughout the cell cycle
163 while loading outside mitosis does not occur in control cells (Fig. 2D-E). In conclusion,
164 overexpression of the CENP-A-specific chaperone CAL1 uncouples CENP-A centromeric
165 loading from mitosis and leads to an uncontrolled overload of CENP-A at centromeres.
166 Importantly, these live cell analyses revealed that CAL1-overexpressing cells underwent
167 mitosis faster than control cells (Fig. 2A).
168 To confirm this observation, we performed time-lapse microscopy experiments in cells
169 overexpressing CAL1 together with H2B-GFP and mCherry-Tubulin. Indeed, we found that
170 mitosis duration, defined as the time between partial nuclear envelop breakdown (NEB) and
171 anaphase entry, was 10 % shorter in CAL1-overexpressing cells as compared to control cells
172 (Fig. 2F-G; videos 3-4). Of note, CAL1 overexpressing cells did neither exhibit more mitotic
173 defects (Fig. S2A) nor did they recruit more endogenous kinetochore proteins (CENP-C,

174 Spc105R, BubR1) during prometaphase (Fig. S2B). CAL1-overexpressing cells also display a
175 functional SAC, since cells treated with the microtubule interfering drug Taxol triggered a cell
176 cycle arrest in prometaphase in control cells as well as in CAL1-overexpressing cells (Fig. S2C-
177 D). We concluded that CAL1-overexpressing cells not only incorporated more CENP-A at
178 centromeres, they also progressed faster through mitosis. We therefore wondered next if
179 CENP-A levels could regulate mitosis duration.
180
181 **CENP-A levels correlate with mitosis duration.**
182 To test the relationship between centromeric CENP-A abundance and the duration of mitosis
183 we designed a strategy to reduce CENP-A levels without inducing chromosome alignment
184 defects that might arrest mitosis (32). We performed CENP-A RNAi depletion in GFP-CENP-A
185 overexpressing cells, which led to undetectable levels of endogenous CENP-A while small
186 amounts of GFP-CENP-A remained in some cells (Fig. 3A-B) and allowed them to go through
187 mitosis (Fig. 3C). Mitosis duration was extended in these cells with reduced CENP-A in
188 comparison to control cells (Fig. 3C-D; videos 5-6). Similar observations have been reported
189 in heterozygous CENP-A mutant fly embryos (33), supporting the hypothesis that CENP-A
190 levels control mitotic length.
191 We next sought to determine if elevated CENP-A levels alone (without CAL1 overexpression)
192 could also influence mitosis duration. However, upregulation of CENP-A to high levels is
193 associated with ectopic CENP-A incorporation into chromosome arms and subsequent defects
194 in mitosis (24). In order to avoid these detrimental effects, we induced CENP-A
195 overexpression from pMT-CENP-A-GFP plasmid with a short and very low $CuSO_4$ pulse (2
196 hours). Under those conditions, CENP-A-GFP was over-expressed while endogenous CENP-A
197 levels were decreased leading to an overall increased CENP-A levels (Fig. 3E). However, 22

198 hours after the $CuSO_4$ pulse untagged CENP-A was almost undetectable, suggesting that cells
199 have a homeostatic mechanism that controls the total abundance of CENP-A protein (Fig. 3E).
200 Under these conditions, non-centromeric CENP-A was undetectable (Fig. 3F) and increased
201 amount of CENP-A-GFP localized to centromeres (Fig. 3G-H). Using time-lapse analysis, we
202 found that cells with increased centromeric CENP-A levels progressed significantly faster
203 through mitosis without increased segregation defects (Fig. 3I-K; videos 7-8). Together these
204 results further suggest that centromeric CENP-A levels influence mitosis duration.
205
206 **CENP-A loading correlates with mitosis duration.**
207 CENP-A loading peaks during prometaphase-metaphase in *Drosophila* S2 cells. Therefore, we
208 hypothesized that the amount of newly synthesized CENP-A that can be incorporated into
209 centromeric chromatin depends on mitosis duration. Mitosis progression is controlled by the
210 action of SAC proteins, which delay entry into anaphase until all chromosomes are properly
211 attached and aligned at the metaphase plate. We depleted two mitotic checkpoint proteins,
212 BubR1 and Mad2, known to reduce mitosis duration (34-36). These depletions (Fig. S3A) led
213 to a decrease of newly synthesized centromeric SNAP-CENP-A incorporation (Fig. 4A-B). In
214 contrast, depletion of Mis12 (Fig. S3A), which has been previously shown not to affect
215 duration of mitosis in Drosophila cultured cells (37), did not alter SNAP-CENP-A amount at
216 centromeres (Fig. 4A-B). Extending metaphase duration by preventing entry into anaphase
217 through depletion of Spindly (required for silencing of the SAC) (38) or of the APC/C cofactor
218 Cdc27 (39)(Fig. S3A) did not cause an increase of CENP-A levels at centromeres when
219 compared to control (Fig. 4A-B), further confirming that loading occurs prior to anaphase (10).
220 Irreversibly arresting cells in prometaphase by the microtubule-depolymerizing drug
221 Nocodazole or in metaphase by the proteasome inhibitor MG132 also did not cause changes

222 in newly synthesized SNAP-CENP-A levels at centromeres (Fig. S3B-C). SNAP-CAL1
223 centromeric levels were similarly affected: an acceleration of mitotic timing by BubR1 or
224 Mad2 RNAi led to a decrease of loading, whereas mitotic arrest by Cdc27 or Spindly RNAi did
225 not affect it (Fig. S3D). This set of experiments suggests that the amount of new CENP-A
226 molecules that are incorporated into centromeric chromatin is limited at each round of
227 mitosis and the length of mitosis directly correlates with the amount of centromerically
228 loaded CENP-A (Fig. 4C).
229
230 **RZZ component Zw10 interacts with centromeric proteins.**
231 In order to identify a putative connection between CENP-A loading and mitosis progression,
232 we performed a targeted Yeast-two-hybrid screen using either CAL1 or CENP-A as bait and
233 known SAC proteins as prey. These experiments showed that the RZZ component Zw10
234 weakly but consistently binds to full length CAL1 and CENP-A (Fig. 4D). To identify the domains
235 of each protein required for the interaction, we repeated the YTH analysis with fragments of
236 CAL1 and Zw10. This analysis revealed a strong interaction of the C-terminus of Zw10 (amino
237 acids 482-721) with the C-terminus of CAL1 (amino acids 680-979) (Fig.S4A), the same domain
238 of CAL1 that also binds CENP-C and Roadkill (Fig. S4B) (29, 30). No further interactions were
239 detected between the other checkpoint proteins and the centromeric proteins suggesting
240 that Zw10 might be the key component that connects centromere loading to the checkpoint
241 proteins and ultimately mitosis duration. Our analysis regarding Bub1 has been inconclusive
242 due to self-activation of the Bub1 construct (blue color in the control transformation) but the
243 absence of interaction between CAL1 and Bub1 has been reported previously (30). To validate
244 the interaction between Zw10 and the centromeric proteins, we expressed and purified GST-
245 Zw10, His-CAL1 and His-CENP-A in bacteria. Pulldown experiments using those proteins

246 confirmed that Zw10 directly binds CAL1 (Fig. 5A). We did not detect any interaction between
247 GST-Zw10 and HIS-CENP-A (Fig. S4C). To further confirm the interaction in cells, we
248 established a cell line overexpressing GFP-tagged Zw10. Firstly we confirmed that GFP-Zw10
249 localization in cultured cells (Fig. S4D) is in accordance with endogenous protein (40-43) as
250 well as transgene expression (44) reported in *Drosophila* tissues: following the disassembly of
251 the nuclear envelope at the onset of mitosis Zw10 was recruited to the kinetochore where it
252 remained until complete chromosome biorientation. GFP-Zw10 was then transported along
253 the spindle microtubules in a process mediated by Spindly and dynein required to silence the
254 SAC (38, 45-47). We next performed immunoprecipitations experiments, which showed that
255 CAL1 co-immunoprecipitated with GFP-Zw10 (Fig. 5B), confirming our pull-down and yeast
256 two hybrid experiments. We concluded from this set of experiments that CAL1 interacts with
257 Zw10, and that this interaction may be involved in coordinating CENP-A centromeric loading
258 with mitosis progression.
259
260 **Zw10 affects the loading of newly synthesized CENP-A during mitosis.**
261 The RZZ complex recruits the MAD proteins to the kinetochore, and is thus essential for the
262 SAC (44, 48). Therefore, we sought to determine if Zw10 depletion could recapitulate the
263 effects observed consecutive to the depletion of the other SAC proteins (Fig. 4A-B). Indeed,
264 Zw10 depletion led to a 30 % reduction of newly synthesized SNAP-CENP-A (Fig. 5C-D) and
265 SNAP-CAL1 (Fig. S5A-B) at centromeres compared to control-depleted cells. Time-lapse
266 microscopy analysis of cells stably expressing H2B-GFP and mCherry-Tubulin confirmed that
267 mitotic timing was significantly shorter in Zw10-depleted cells than in control cells (Fig. 5E-F;
268 videos 9-10). This result is in accordance with the Premature Sister Chromatids Separation
269 (PSCS) phenotype observed in Zw10 mutant embryos and larval tissues (41, 49, 50).

270 To exclude a potential role of Zw10 in CENP-A stability we performed a SNAP-tag pulse chase
271 experiment (Fig. S5C-D) that showed that centromeric SNAP-CENP-A was not affected by
272 Zw10 depletion. Furthermore, FRAP analysis revealed that the recovery rate of GFP-CENP-A
273 at centromeres was comparable in control and Zw10-depleted cells (Fig. S5E-F). Thus, the
274 CENP-A mitotic loading machinery was functional in Zw10-depleted cells suggesting that Zw10
275 does not influence CENP-A loading directly but through its role in checkpoint activity.
276
277 **Zw10 mediates the recruitment of the RZZ to the kinetochore independently of Spc105R.**
278 How RZZ is recruited to the kinetochore at mitosis onset remains elusive in *Drosophila*. We
279 first sought to determine if one of the RZZ components is responsible for targeting the whole
280 complex to the kinetochore. We established cell lines overexpressing GFP-ROD and GFP-
281 Zwilch and confirmed that the localization of the tagged proteins is consistent with previous
282 reports (44, 49, 51, 52) (Fig. S4E-F). Knockdown of RZZ complex components (Fig. S6A) led to
283 the expected spindle morphology defects in all cell lines (Fig. 6) (41, 52-54). Importantly,
284 depletion of any complex component led to a reduction of the other GFP-RZZ proteins at
285 kinetochores (Fig. 6) suggesting that the RZZ components are mutually dependent on each
286 other similar to what has been reported in Drosophila tissues (40, 42, 52, 54, 55). However,
287 levels of GFP-Zw10 at kinetochores were the least affected indicating that some GFP-Zw10 is
288 still recruited to kinetochores in the absence of its complex partners ROD or Zwilch (Fig. 6C),
289 suggesting that Zw10 is the most proximal component of the complex at kinetochores in
290 Drosophila cells. Like all kinetochore proteins tested so far (56), the localization of Zw10 to
291 the kinetochore is abolished when CENP-A (Fig. 7B-C) and/or its loading factor CAL1 (Fig. S6B)
292 are depleted, even though Zw10 protein levels remained largely unchanged (Fig. 7A).
293

294 In mammalian cells, several pathways have been implicated in the recruitment of the RZZ
295 complex including KNL1, Bub1 and Zwint (57-61). As no ortholog of Zwint has been identified
296 in *Drosophila* so far, we tested if the *Drosophila* KNL1 ortholog Spc105R or Bub1 are required
297 for RZZ recruitment to the kinetochore. Depletion of Spc105R (Fig. S6A) did not affect Zw10
298 localization (Fig. 6C-D), nor did Bub1 depletion (Fig. 6C and S6A, S6C). We also tested Mis12,
299 which has been shown to localize to kinetochores throughout the cell cycle (56) and found
300 that it is also not involved in Zw10 recruitment to the kinetochore (Fig. 6C and S6A, S6D).
301 Since the recruitment of KMN network depends the prior localization of Spc105R and Mis12
302 at kinetochores (56), those knockdown experiments suggest that the RZZ recruitment to the
303 kinetochore is independent of the KMN network. Conversely, depletion of Zw10 (Fig.7A) did
304 not prevent Spc105R (Fig. 7E-F), Mis12 (Fig. S6E-F), Ndc80 (Fig. 7G-H) or BubR1 (Fig. S6G-H)
305 localization to the kinetochore. Therefore, we propose that the *Drosophila* checkpoint
306 proteins and outer kinetochore components are assembled through two independent
307 branches: on the one hand, CAL1 directly recruits the RZZ complex, which is necessary to
308 localize the MAD proteins to the kinetochore (44, 48), and on the other hand, CENP-C attracts
309 Mis12-Spc105R, which are required to recruit all others components of the KMN network as
310 well as the BUB proteins (28, 56, 62-64). We conclude from these results that there is a direct
311 connection of the SAC and the loading of CENP-A by CAL1, and that the CAL1-RZZ branch
312 directly affects CENP-A loading and mitotic duration, thereby controlling CENP-A loading in a
313 time-dependent manner.
314

315 **Discussion**

316 Centromeric chromatin has been shown to behave differently to non-centromeric chromatin
317 in several ways, for instance CENP-A replenishment after DNA synthesis is replication-

318 independent, which depends on specialized loading factors. In *Drosophila* cells, CENP-A
319 loading takes place primarily during prometaphase-metaphase (10). Additional turnover of
320 CENP-A in G1 has been reported leading to the hypothesis that CENP-A could be further
321 incorporated at this stage (12). We did not observe any CENP-A turnover during early G1 in
322 our FRAP experiments when we bleached centromeric CENP-A at the end of cytokinesis.
323 However, our FRAP experiments and our live staining of newly synthesized SNAP-CENP-A
324 confirmed the observations reported by Mellone et al., that the majority of CENP-A loading
325 takes place during mitosis in *Drosophila* cultured cells (10).

326 In flies, CENP-A incorporation is controlled by its chaperone CAL1 (18, 20, 30). We found that
327 overexpression of CAL1 leads to increased CENP-A protein levels. Under our conditions, CAL1-
328 V5 was strongly overexpressed and caused an intense centromeric and nucleolar localization
329 of CAL1 and a centromere-specific overload of CENP-A. However, ectopic incorporation of
330 CENP-A was never observed suggesting that CAL1 loads CENP-A exclusively to centromeres
331 and that ectopic CENP-A incorporation in flies depends on alternative loading mechanisms
332 similar to what has been suggested in human cells (65). Importantly, increased centromeric
333 CENP-A levels following CAL1 overexpression did not cause chromosome segregation defects
334 but correlated with faster mitosis. A similar acceleration of mitotic timing was observed when
335 CENP-A was overexpressed in a controlled manner that did not lead to massive incorporation
336 at ectopic sites, revealing a possible link between CENP-A loading and mitotic timing. Indeed,
337 shortening mitosis duration by depleting Mad2 or BubR1 (66) was associated with decreased
338 CENP-A loading. Elongating the mitotic time window during which CENP-A is usually loaded
339 (Spindly or Cdc27 depletion, or by drug treatment) did not increase the amount of CENP-A
340 incorporated at centromeres, showing that the length of mitosis alone is insufficient to
341 control CENP-A amounts at centromeres but that only a defined amount of CENP-A can be

342 incorporated at each mitosis, which probably correlates with the available levels of CAL1.
343 Indeed, live analysis of CAL1-overexpressing cells allowed us to visualize newly synthesized
344 CENP-A incorporation to centromeres in all stages of the cell cycle. This strongly suggests that
345 CAL1 controls CENP-A incorporation into centromeric chromatin both quantitatively and
346 temporally. How exactly CENP-A levels at centromeres are sensed is unclear but we identified
347 the RZZ-component Zw10 as a new CAL1 interacting partner, which directly connects CENP-A
348 loading to the SAC. Therefore, we suggest the following model: efficient CENP-A loading by
349 CAL1 during mitosis recruits ZW10 up to a threshold, which is sensed by the SAC. Elevated
350 levels of CENP-A or CAL1, therefore, would accelerate RZZ recruitment and shorten mitosis.
351 It has previously been proposed that BubR1 and Mad2 function as mitotic timer (35, 36, 66,
352 67). Mad2 but not Mad1 has been shown to be a central determinant of the mitotic timing
353 (66, 68), leading to the hypothesis that cytosolic Mad2-Cdc20 complexes form independently
354 of Mad1 and determine the timing of mitosis (68, 69). Low CENP-A levels at centromeres could
355 lead to more cytosolic Mad2 thereby keeping the timer active longer (33). We hypothesized
356 that higher CENP-A levels at centromeres during early mitosis would accelerate the
357 recruitment of RZZ and consequently Mad2 to the kinetochores, therefore, releasing the
358 timer and shortening mitosis duration in cells where kinetochores attach properly to the
359 spindle microtubules. Interestingly, Nocodazole treatment did not affect CENP-A loading
360 confirming previous observations that kinetochores attachment to the microtubule spindle
361 does not play a role in CENP-A loading (10). These results are pointing further to an additional
362 function of the SAC independent of the control of microtubule attachment. Interestingly,
363 recent evidence shows that RZZ together with Spindly plays a central role in kinetochore
364 expansion during early mitosis to form a fibrous corona that then compacts upon microtubule

365 capture (70-72). Whether and -if so- how the kinetochore expansion by RZZ and spindly is
366 involved in CENP-A loading needs to be investigated in the future.

367

368 Many essential components of the SAC require outer kinetochore components for their
369 localization to centromeric regions. In yeast and worms, for instance, Mad1/2 recruitment
370 depends on KNL1 (73, 74). In other eukaryotes, Mad1/Mad2 recruitment to the kinetochore
371 also requires the RZZ complex (58, 59, 75). In mammalian cells, RZZ recruitment to the
372 kinetochore depends on Bub1, which itself requires KNL1/Zwint (59, 61, 76) although some
373 data suggest the existence of a KNL1-independent mechanism (59, 75, 77). Several outer
374 components are missing from the *Drosophila* kinetochore (56, 78) and even though Mad1/2
375 recruitment to the kinetochore depends on the RZZ complex (48), the factors necessary for
376 the localization of the RZZ to kinetochores are unknown. We showed here that RZZ
377 localization to the kinetochores does not require KNL1^{Spc105R} but depends on the centromeric
378 proteins CAL1 and CENP-A. Therefore, we propose that the *Drosophila* outer kinetochore and
379 components of the SAC assemble through two independent pathways: the CENP-C-KMN-
380 Bub1-Bub3/BubR1 branch (28, 62, 64) or the CAL1-RZZ-Mad1/2 branch. How those two
381 pathways communicate for the formation of MCC complexes remains to be determined. One
382 link may be the KMN complex, since Mad2 has been shown to be diminished in the absence
383 of KMN proteins (37). Interestingly, Spc105R mutation does not affect SAC function in fly
384 embryos suggesting that flies rely more on the RZZ-Mad1/2 branch to engage the SAC (62).

385 CENP-A expression (79) and its stability (23, 29) together with its dependence on the low
386 abundant and highly specific loading factor CAL1 and the here shown connection to mitotic
387 events are likely interconnected cellular surveillance mechanisms to avoid misincorporation

388 of CENP-A and, therefore, securing genome stability. How CAL1 itself is regulated to obtain
389 such specificity is currently unknown. In conclusion, we show that there is a direct crosstalk
390 between the SAC and the maintenance of centromeric chromatin, ensuring mitotic fidelity
391 not only by controlling microtubule attachment but also by regulating accurate composition
392 of centromeres.

393

394 **Materials and methods**

395 **Gene constructs**

396 Plasmid encoding CENP-A tagged with a N-terminal EGFP has been described previously (20)
397 as well as those encoding CENP-A and CAL1 with N-terminal SNAP tag (10). Constructs created
398 for this study (GFP-ROD, GFP-Zwilch, GFP-Zw10) were cloned into AscI and PacI sites of the
399 pCopia–localization and purification (LAP) vector with a basal expression Copia promoter and
400 an N-terminal mEGFP tag (20). For overexpression studies, CAL1-V5 and CENP-A-GFP were
401 cloned into pMT vector (Invitrogen). For yeast two hybrid studies, pMM6 plasmids containing
402 full length CAL1, CAL1 truncations and CENP-A have been described in (29). Bub1, Bub3,
403 BubR1, Mad1, Mad2, Zw10 (full length, aa1-240, aa241-481, aa482-721), Zwilch and Rod (full
404 length, aa1-696, aa697-1392, aa1393-2090) were cloned into pMM5 plasmids. For bacterial
405 expression, pCA528 plasmids containing CAL1 and CENP-A have been described in (29). Zw10
406 was cloned into pGEX5x-1.

407 **Cell culture**

408 Cell maintenance

409 *Drosophila* S2 cells were maintained under sterile conditions at 25°C in Schneider medium
410 containing 10 % heat-inactivated fetal bovine serum (FBS) and 100 µg/ml
411 Penicillin/Streptomycin. Expression of genes under the metallothionein promoter (pMT
412 vector) was induced by supplementing the medium with $CuSO_4$ (CENP-A-GFP: 10 µM for 2 h;
413 CAL1-V5: 100 µM for 24 h).

414 RNAi and Transfection Experiments

415 Double-stranded RNA (dsRNA) was produced using the MEGAscript (Ambion) kit according to
416 the manufacturer's protocol. RNAi was carried out as described previously (20). In short, 10^6
417 S2 cells were incubated for 1 h with 15 µg dsRNA in serum-free medium. Subsequently, 2
418 volumes of 15 % serum containing medium were added. Analysis was usually performed 96 h
419 after treatment.

420 Stable cell lines were generated by co-transfecting the plasmid of interest together with a
421 plasmid carrying the resistance gene for hygromycin with Cellfectin II (Life Technologies), and
422 the selection process was started 2 d after transfection by supplementing the media with 250
423 µg/ml Hygromycin B.

424 SNAP quench chase pulse experiments

425 Cells overexpressing either SNAP-tagged CENP-A or CAL1 proteins were treated with dsRNA
426 as described in RNAi section. After 3 days, cells were collected and incubated in fresh SM
427 containing 10 µM SNAP-Cell Block (New England Biolabs S9106), for 30 min at 25°C, 400 rpm.
428 Cells were then pelleted, washed 3 times (1st wash for 30 min, at 25°C, 400 rpm) and plated
429 in conditional medium. After 24 h, cells were collected and incubated with 4 µM SNAP-Cell
430 TMR-Star (New England Biolabs S9105) or SNAP-SiR647 (New England Biolabs S9102) for 15
431 min at 25°C, 400 rpm, protected from light. The cells were then pelleted, washed 3 times with

432 SM (1st wash for 30 min, at 25°C, 400 rpm), one time in PBS and prepared for imaging. Cells
433 were settled on a glass coverslip for 10 min, fixed with 4 % PFA for 10 min, washed three times
434 in PBS, and counterstained with DAPI before mounting.

435 SNAP pulse-chase

436 Cells overexpressing either SNAP-tagged CENP-A or CAL1 proteins were treated with dsRNA
437 as described in RNAi section. After 3 days, cells were collected and incubated in fresh medium
438 containing 4 µM SNAP-Cell TMR-Star (New England Biolabs, Inc.) for 15 min at 25°C, 400 rpm,
439 protected from light. Cells were then washed 3 times with SM (1st wash for 30 min, at 25°C,
440 400 rpm) and plated in conditional medium. After 24 h, cells were collected and prepared for
441 imaging as previously described.

442 SNAP live imaging

443 To follow incorporation of newly synthesized SNAP-CENP-A, SNAP-CENP-A was blocked as
444 previously described (see section SNAP quench chase pulse). Cells were then resuspended in
445 conditional medium containing 0.5 µM SNAP-640 dye (31) and placed into an Ibidi imaging
446 chamber before imaging.

447 **Immunofluorescence**

448 IF was essentially performed as described previously (20). Cells were harvested, washed once
449 with PBS and placed to settle on a glass coverslip for 10 min before fixation with 4 % PFA for
450 10 min. Cells were washed three times in PBS and permeabilized for 5 min with PBS containing
451 with 0.5 % Triton X-100. Unspecific binding was prevented by blocking the cells for 30 min
452 with 1 % BSA in PBS. Primary antibodies diluted in blocking solution were incubated for 30
453 min at RT. After three washes with PBS, cells were incubated with the corresponding,
454 fluorescently labeled secondary antibodies (diluted in blocking solution) for 30 min at RT. The

455 secondary antibody incubation and all the following steps were performed while protected
456 from light. After three washes in PBS, DNA was stained for 5 min with DAPI (1 µg/ml in PBS).
457 The cells were then washed two more times with PBS before mounting in Aqua/Polymount
458 medium (Polysciences, Inc.) on a glass slide.

459 **Preparation of mitotic chromosome spreads**

460 Mitotic chromosome spreads were essentially performed as described previously (80). To
461 obtain mitotic chromosomes, $2x10^5$ exponentially growing cells were arrested in mitosis with
462 2.5 µg/µl Colcemid for 1 h, centrifuged for 3 min at 800 *g*, resuspended in 0.5 ml hypotonic
463 sodium citrate solution (0.5 % Na-citrate in ddH2O), and incubated for 8–10 min. Cells were
464 spun on positively charged slides in a cytocentrifuge (Shandon 4 Cytospin; Thermo Fisher
465 Scientific) at 900 rpm for 10 min. Slides were placed 10 min in KCM buffer (120 mM KCl, 20
466 mM NaCl, 10 mM Tris-HCl ph7.7, 0.1 % Triton X-100) before 30 min incubation with primary
467 antibodies diluted in TEEN buffer (1 mM Triethanolamine: HCl pH8.5, 0.2 mM EDTA, 25 mM
468 NaCl, 0.1 % TX-100, 0.1 % BSA) at 37°C. After 3 washes in KB buffer (10 mM Tris-HCl pH7.7,
469 0.15 M NaCl, 0.1 % BSA) at RT, slides were incubated with secondary antibodies diluted in
470 TEEN buffer for 30 min at 37°C. Slides were then washed 3 times in KB before incubation with
471 1 µg/ml DAPI diluted in PBS for 5 min at RT. Slides were then mounted in Aqua/Polymount
472 medium (Polysciences, Inc.).

473 **Microscopy and Image analysis**

474 All Images were acquired on a DeltaVision Core system (Applied Precision) equipped with an
475 Olympus UPlanSApo 100X oil immersion objective (n.a. 1.4) at binning 1x1 (mitotic figures) or
476 2x2 (interphase). If not stated otherwise, images were taken as z stacks of 0.3 µm increments.
477 All images were deconvolved (20 cycles additive with noise filtering) and maximum-projected

478 using the Applied Precisions soft-WoRx 3.7.1 suite. Image quantification was done using
479 ImageJ software. For determining the number and intensities of centromere/kinetochore
480 dots, a set of plugins developed by the Nikon Imaging Centre, University Heidelberg was used.
481 After marking the nuclear boundaries in the DAPI channel and saving them with the ROI tool,
482 the spots in the channel of interest were enhanced using the DoG spot enhancer plugin. The
483 threshold was adjusted using ‘‘Li’’ instead of default settings. The number of spots with their
484 mean intensities relative to the nuclear area was determined using the ROI particle analyzer
485 plugin.
486 Time-lapse imaging was performed on a DeltaVision Core system (Applied Precision)
487 equipped either with an Olympus 60X/1.42, N Plan Apo oil immersion objective or an Olympus
488 40X/1.35, UApo/340 oil objective, at binning 2x2 with 3 min (mitosis duration and fidelity
489 measurements) or 15 min (SNAP-CENP-A live imaging) time-lapse series, for 16 h, with z stacks
490 of 1 µm increment.
491 FRAP was performed on a Zeiss LSM 780 confocal microscope equipped with a 63x/1.4 oil
492 immersion objective. Number of focal planes per time point, as well as time intervals and total
493 duration were adjusted according to experimental needs. The spacing of focal planes was 1
494 µm in all experiments. Recovery of EGFP-CENP-A signal was analyzed using FRAP analysis
495 plugin developed by ZMBH imaging facility. After marking the boundaries of the cell of
496 interest, the threshold allowing visualization of centromeric signal exclusively was defined on
497 pre-bleach image. Total intensity of the thresholded signal was then measured for each time
498 point as well as the area. Similar measurements were performed on non-bleached cells from
499 the same area to determine the photobleaching level in each time-series. After correction,
500 EGFP-CENP-A signal intensity was plotted against the time, a linear regression curve was
501 fitted.

502 **Protein purification and GST-pulldown**

503 Zw10 coding sequence was cloned into pGEX5x-1 bacterial expression vector and transformed
504 into BL21DE3 bacteria. Expression was induced by addition of 1 mM IPTG at OD = 0.6. After
505 16 h at 21°C, bacteria were pelleted and resuspended in lysis buffer (1 % TX100, 1 mM DTT, 1
506 mg/ml Lysozyme, 2 mg/ml aprotinin, 5 mg/ml leupeptin, 1 mg/ml pepstatin in PBS). After 30
507 min incubation at 4°C, bacteria were sonicated (10 cycles, 30 seconds pulse-30 seconds pause,
508 60 % output power). The lysate was then centrifuged at 15000 g for 45 min. The supernatant
509 was then incubated with Protino glutathione-agarose 4B (Machery-Nagel) for 1 h at 4°C. After
510 6 washes with 1 % TX100 in PBS, GST-Zw10 was eluted with 20 mM reduced glutathione, 50
511 mM Tris-HCl pH 8, 1 mM DTT. Buffer was then exchanged using Amicon Ultra 50 K with
512 storage buffer (50 mM Tris-HCl pH 8, 1 mM DTT). His-Sumo-CAL1 and His-Sumo-CENP-A
513 purifications have been described in (29).

514 Pulldown assays were performed by incubating GST or GST-Zw10 coupled beads with 100 ng
515 His-Sumo-CAL1 or His-Sumo-CENP-A in interaction buffer (20 mM Tris pH 8, 150 mM NaCl, 0.5
516 mM EDTA, 10 % glycerol, 0.1 % NP-40, 1 mM DTT) for 1 h at 4°C. Beads were then washed 6
517 times in interaction buffer before resuspension in 1 bead volume 2X sample Laemmli buffer
518 and boiling at 95°C for 5 min.

519 **Immunoprecipitation**

520 GFP-tagged proteins were isolated using a GFP-specific single chain antibody (GBP) coupled
521 to NHS-activated Sepharose (GE) (81). A total of 1.0–2.0 x 10^8 cells were lysed in two pellet
522 volumes of 20 mM Tris-HCl pH 7.5, 1 % NP-40, 250 mM NaCl, 20 mM NEM, 10 mM NaF, 2 mM
523 PMSF, 2 mg/ml aprotinin, 5 mg/ml leupeptin, 1 mg/ml pepstatin for 15 min at 4 °C. After
524 clearing the lysate by centrifugation, the supernatant was incubated for 2 h at 4 °C with 50 µl

525 pre-equilibated GBP-beads. The beads were washed six times with lysis buffer and eluted with
526 2x Laemmli buffer 5 min at 95°C.

527 **WB analysis and quantification**

528 Cell lysates were separated on a 4-15 % SDS poly-acrylamide gel, transferred onto a
529 nitrocellulose membrane for 2 h at 100 V (Tris-Glycin buffer containing 0.1 % SDS). After
530 blocking in 5 % milk in PBST, primary antibodies were incubated O/N at 4°C in the blocking
531 solution. After washing, secondary antibodies coupled to horseradish peroxidase were added
532 for 1 h at RT before ECL detection (Thermo Fisher Scientific). Immunoblots were quantified
533 using ImageJ.

534 **Antibodies**

535 The following primary antibodies were used: rabbit H3 (Abcam AB 1791), rabbit CAL1 (29),
536 chicken CENP-A (Erhardt lab + 20), rabbit CENP-A (Active Motif 39713), rabbit YFP (from Pr.
537 Bukau), mouse tubulin (Sigma T9026), mouse V5 (Invitrogen V8012), sheep Scp105R (from Dr.
538 Glover), rabbit Zw10 (from Dr. Goldberg), guinea pig CENP-C (20), rabbit phospho-S10 histone
539 H3 (Abcam ab5176), BubR1 (from Dr. Glover), goat GST (GE healthcare 27457701), rabbit His
540 (Abcam ab9108), rabbit Ndc80 (82), rabbit Mis12 (82). Secondary antibodies coupled to Alexa
541 Fluor 488, Alexa Fluor 546 and Alexa Fluor 647 fluorophores (Molecular Probes) were used
542 for IF, and horseradish peroxidase-conjugated secondary antibodies (Sigma) were used for
543 WB analysis.

544 **Reverse transcription and Quantitative qPCR**

545 RNA was isolated using Trizol(R) according to the manufacturer's procedures. Whole genome
546 cDNA synthesis was performed using the Quantitect Reverse Transcription kit (Invitrogen),

547 with a combination of oligo (dT) and random hexamer primers in equal proportions. A control
548 reaction with no reverse transcription was always performed in parallel.

549 qPCR was performed after cDNA synthesis on a LightCycler 480 (Roche) using LightCycler 480
550 SYBR Green I Master (Roche). All reactions were run in triplicate in a LightCycler 480 multiwell
551 plate. Actin was used as a reference. The level of each targeted gene in the control mock-
552 treated sample was normalized to 1, and compared with the corresponding–depleted
553 samples.

554 **Yeast two hybrid**

555 Protein-protein interactions were tested using pMM5 and pMM6 fusion constructs and the
556 yeast strain SGY37VIII. The YTH was performed as described previously (83). In short,
557 interactions were judged based on the activity of β-galactosidase that results in the
558 conversion of X-Gal (5-bromo-4-chloro-3-indolyl-b-D-galactosidase) into a blue dye.

559

560 **Acknowledgements:**

561 We thank B. Bukau, D. Glover, M. Przewloka, M. Goldberg, R. Karess for antibodies and
562 constructs, V. Belov, A. Butkevich and the Facility of synthetic chemistry of the Max Planck
563 Institute for Biophysical Chemistry (MPIBPC) for the gift of the compound 640SiRH-BG. We
564 thank the ZMBH Imaging Facility and A. Jafar Pour for ImageJ FRAP analysis plugins; H. Lorenz
565 for help with imaging, R. Vlijm and the Erhardt laboratory members for discussions; E.
566 Schiebel and S. Corless for critical comments on the manuscript. We acknowledge funding
567 from the Deutsche Forschungsgemeinschaft through the grant EXC81 (CellNetworks),

568 ER576/2-2, SFB1036, the European Research Council through the grant ERC-CoG-682496
569 (cenRNA) to SE. ALP is an alumna of the CellNetworks postdoc program.

570

571 Competing interests: No competing interests declared

572

573

574 **Figures legends**

575 **Figure 1: CAL1 overexpression leads to increased CENP-A levels at centromeres.**

576 **A.** Immunofluorescence of CAL1-V5 expressing cells. CAL1-V5 expression was induced by
577 addition of 100 µM $CuSO_4$ for 24 h. Cells were fixed and stained with anti-V5 antibody (green).
578 DNA was counterstained with DAPI. The percentage of transfected cells displaying either type
579 of localization is shown. **B.** Immunoblot of CAL1-V5 expressing cells treated as in A. Anti-CAL1
580 (endogenous CAL1 and CAL1-V5) and anti-H3 antibodies were used. **C.** Quantification showing
581 CAL1 centromeric signal intensity per nucleus as % of non-induced control cells. **D.**
582 Immunoblot of CENP-A (either GFP or SNAP N-terminally tagged) expressing cells with or
583 without concomitant CAL1 overexpression. Anti-V5 (CAL1-V5), anti-CENP-A (endogenous
584 CENP-A and tagged-CENP-A) and anti-H3 antibodies were used. The graph shows CENP-A level
585 in each cell line as fold change from baseline levels determined in protein extracts from S2
586 cells (N=4). **E.** Metaphase chromosomes of CAL1-V5 expressing cells treated as in A.
587 Metaphase chromosomes were stained with anti-CENP-A antibody. DNA was counterstained
588 with DAPI. Scale bar 1 µm. **F.** Immunofluorescence of CAL1-V5/GFP-CENP-A expressing cells
589 treated as in A. Cells were fixed and stained with anti-CENP-C antibody (red). DNA was
590 counterstained with DAPI. **G.** Quantification of F. GFP-CENP-A and CENP-C signal intensities
591 per centromere were measured and are shown as % of non-induced control cells. **H.** Time line
592 of induction experiment followed by a Quench-Chase-Pulse SNAP-tag experiment. After 24 h
593 CAL1-V5 induction, cells were incubated with SNAP-Block to quench existing SNAP-CENP-A
594 molecules (Q), washed and cultured for 24 h. After 24 h chase in presence of $CuSO_4$, cells were
595 incubated with SNAP-SiR647 (red) to stain newly synthesized SNAP-CENP-A molecules (P). The
596 images show representative immunofluorescence staining of SNAP-CENP-A expressing cells

597 in control and CAL1 overexpressing cells. DNA was counterstained with DAPI. **I.** Quantification
598 of G. SNAP-CENP-A signal intensity per centromere was measured and is shown as % of non-
599 induced control. All graphs show Mean +/- SEM of 3 experiments (n>300 cells), Student t-test
600 (*n.s.*: non-significant; *: p<0.05; **: p<0.01, ***: p<0.001). Scale bar= 2 µm.

601

602 **Figure 2: Overexpression of CAL1 leads to CENP-A centromeric loading outside of mitosis.**

603 **A.** FRAP experiments of GFP-CENP-A in mitosis in CAL1-overexpressing cells. CAL1-V5
604 expression was induced for 24 h. GFP-CENP-A signal was partially bleached in prophase and
605 cells were imaged until telophase. Time lapse: 90 s. Scale bar= 2 µm. **B.** Quantification of A.
606 The total GFP-CENP-A centromeric signal is shown as mean +/- SEM, n≥ 11 cells. **C.** Time-lapse
607 imaging of SNAP-CENP-A/mCherry-Tubulin cells with or without concomitant overexpression
608 of CAL1. CAL1-V5 expression was induced for 24 h. The cells were then incubated with SNAP-
609 Block to quench existing SNAP-CENP-A molecules, washed and resuspended in conditional
610 medium containing 0.5 µM SNAP-640 dye. Cells were imaged for 16 h to visualize newly
611 synthesized SNAP-CENP-A. Time lapse 15 min. Scale bar= 2 µm. Intensity levels have been
612 adjusted separately for each condition. **D-E.** Quantifications of C. **D.** Table showing the % of
613 SNAP-CENP-A positive cells (+ cells) and the timing of loading. **E.** For each cycling cell, the
614 earliest detection time point of SNAP-CENP-A (Y-axis) is plotted versus the time of cytokinesis
615 (X-axis). t0 on both axes corresponds to start of imaging after SNAP-Block. **F.** Time-lapse
616 imaging of H2B-GFP/mCherry Tubulin cells with or without concomitant overexpression of
617 CAL1. CAL1-V5 expression was induced for 24 h. The cells were imaged for 16 h. Time lapse 3
618 min. Scale bar= 2 µm. **G.** Quantification of F showing the mitosis duration from nuclear
619 envelope breakdown (determined by mCherry-Tubulin nuclear diffusion concomitant to DNA

620 condensation) to anaphase entry. Mean +/- SEM, n>200 cells. Student t-test (*: p<0.05; **:
621 p<0.01, ***: p<0.001).

622

623 **Figure 3: CENP-A levels affects mitosis duration.**

624 **A.** Immunoblot showing CENP-A knockdown efficiency in GFP-CENP-A/mCherry-Tubulin
625 expressing cells. An anti-CENP-A antibody was used to detect endogenous CENP-A and
626 overexpressed GFP-CENP-A. **B.** Quantification showing GFP-CENP-A centromeric signal
627 intensity per nucleus at t0 of time-lapse imaging. Mean +/- SEM, n>80 cells. Student t-test
628 (***: p<0.001). Data from 3 experiments were normalized and combined. **C.** Time-lapse
629 imaging of GFP-CENP-A/mCherry-tubulin expressing cells after CENP-A depletion. After 72 h
630 dsRNA treatment, cells were imaged for 16 h. Time lapse 3 min. Scale bar= 2 µm. **D.**
631 Quantification of C. showing the mitosis duration of control and CENP-A depleted cells. Mean
632 +/- SEM, n>80 cells. Student t-test (***: p<0.001). **E.** Immunoblot showing CENP-A levels in
633 the different cell lines used. CENP-A antibody detects endogenous and tagged versions of
634 CENP-A. GFP-CENP-A and SNAP-CENP-A are under the constitutive *copia* promoter. CENP-A-
635 GFP expression was induced by activating the *metallothionein* promoter with 10 µM $CuSO_4$
636 for 2 h. Cells were washed and cultured in conditional medium for 22 h. H3 serves as loading
637 control. The graph shows CENP-A level in each cell line as fold change from baseline levels
638 determined in protein extracts from S2 cells (N=4). **F.** Metaphase chromosomes of CENP-A-
639 GFP expressing cells treated as in E. Metaphase chromosomes were stained with anti-CENP-
640 A antibody. DNA was counterstained with DAPI. Intensities have been adjusted separately for
641 each condition. Scale bar= 2 µm. **G.** Immunofluorescence of CENP-A-GFP cells. CENP-A-GFP
642 expression was induced as in E. DNA was counterstained with DAPI. Scale bar= 2 µm. **H.**

643 Quantification of G. showing the total CENP-A-GFP centromeric intensity per nucleus as % of
644 control. Mean +/- SEM of 3 experiments (n>300 cells), Student t-test (***: p<0.001). **I.** Time
645 lapse imaging of cells expressing mCherry-tubulin and inducible CENP-A-GFP. GFP-CENP-A
646 expression was induced by addition of 10 µM $CuSO_4$ to the medium for 2 h. Cells were washed
647 before imaging (16 h). Time lapse 3 min. Scale bar= 2 µm. The intensity levels of CENP-A-GFP
648 in control cells are shown enhanced for visualization purposes. **J.** Quantification of I. showing
649 mitosis duration of control and CENP-A-GFP expressing cells. Mean +/- SEM, n>300 cells.
650 Student t-test (***: p<0.001). **K.** Mitotic phenotypes of CENP-A-GFP/mCherry-Tubulin cells
651 imaged in I. Cells were scored for the accuracy of mitosis: normal or defective (presence of
652 lagging chromosomes in anaphase, formation of tripolar spindles). Mean +/- SEM n > 200
653 cells. Student t-test (*n.s.*: non-significant).

654

655 **Figure 4: CENP-A loading is correlated with mitosis duration.**

656 **A.** SNAP-CENP-A incorporation in BubR1, Mad2, Mis12, Spindly or Cdc27 depleted cells. After
657 72 h dsRNA treatment, a Quench-Chase-Pulse experiment (scheme in Fig. 1H) was performed
658 to stain newly synthesized SNAP-CENP-A molecules (red). DNA was counterstained with DAPI.
659 Scale bar: 2 µm. **B.** Quantification of A. The total SNAP-CENP-A centromeric signal intensity
660 per nucleus is shown as % of control dsRNA-treated cells. Mean +/- SEM of 3 experiments
661 (n>300 cells), Student t-test (*n.s.*: non-significant; ***: p<0.001). **C.** The recovery rate of GFP-
662 CENP-A after photobleaching in mitosis is plotted against the mitosis duration for each
663 analyzed cell. Pearson's correlation test, p<0.01. **D.** Yeast two hybrid interaction tests using
664 SAC proteins as prey with either bait CAL1 or CENP-A. Blue color reflects the interaction
665 between the 2 proteins tested.

666

667 **Figure 5: Zw10 interacts with CENP-A loading factor CAL1.**

668 **A.** ***Left panel.*** Coomassie showing purified GST-Zw10 and His-Sumo-CAL1. ***Right panel.***
669 Immunoblot showing GST-pulldown assays of His-Sumo-CAL1. **B.** Co-immunoprecipitation of
670 CAL1 with GFP-Zw10. GFP (Ctrl) or GFP-Zw10 proteins were immunoprecipitated using the
671 GFP-binding protein (GBP). Pulled down fractions were analyzed by immunoblotting for the
672 presence of CAL1. **C.** SNAP-CENP-A incorporation in Zw10 depleted cells. After 72 h dsRNA
673 treatment, a Quench-Chase-Pulse experiment (scheme in Fig. 1H) was performed to stain
674 newly synthesized SNAP-CENP-A molecules (red). DNA was counterstained with DAPI. Scale
675 bar: 2 µm. **D.** Quantification of C. showing the total SNAP-CENP-A centromeric intensity per
676 nucleus as % of control. Mean +/- SEM of 3 experiments (n>300 cells), Student t-test (***:
677 p<0.001). **E.** Time-lapse imaging of H2B-GFP/mCherry-tubulin expressing cells after Zw10
678 depletion. After 72 h dsRNA treatment, cells were imaged for 16 h. Time lapse 3 min. Scale
679 bar= 2 µm. **F.** Quantification of G showing the mitosis duration. Mean +/- SEM, n>200 cells.
680 Student t-test (***: p<0.001).

681

682 **Figure 6: Zw10 is the most proximal RZZ component at kinetochores in *Drosophila*.**

683 **A. Left panel** Immunofluorescence of cells expressing GFP-Rod in combination with mCherry-
684 Tubulin after depletion of RZZ components. After 96 h dsRNA treatment, cells were fixed and
685 stained with anti-GFP antibody (green) and anti-CENP-A (red), DNA was counterstained with
686 DAPI. ***Middle panel.*** Prometaphase cells were counted for the presence or absence of GFP
687 signal at kinetochores. ***Right panel.*** Quantification showing the total GFP-Rod kinetochore

688 intensity per cell. GFP fluorescence intensity at kinetochores was measured for each cell and
689 then normalized within one experiment allowing pooling of the measurements for at least 3
690 experiments per condition. **B.** Similar experiments as in A were performed in GFP-Zwilch
691 overexpressing cells. **C.** Similar experiments as in A were performed in GFP-Zw10
692 overexpressing cells. Mean +/- SEM, n>100 cells. Student t-test (*n.s.*: non-significant; *:
693 p<0.05; **: p<0.01***: p<0.001). Scale bar= 2 µm.

694

695 **Figure 7: RZZ recruitment to the kinetochore depends on a direct interaction with inner**
696 **centromere proteins.**

697 **A.** Immunoblot showing protein levels after dsRNA treatment. CENP-C, CAL1, Zw10 and CENP-
698 A antibodies were used. H3 serves as a loading control. **B.** Immunofluorescence of GFP-
699 Zw10/mCherry-Tubulin expressing cells after depletion of CENP-A. At day 4 of RNAi, cells were
700 fixed and stained with anti-GFP (green), anti-CENP-A (red) antibodies, DNA was
701 counterstained with DAPI. Scale bar= 2 µm. **C.** Quantifications of B. showing the total GFP-
702 Zw10 centromeric intensity per nucleus as % of control. Prometaphase cells were selected for
703 analysis. Mean +/- SEM of 3 experiments (n>100 cells), Student t-test (*n.s.*: non-significant; *:
704 p<0.05). **D.** Immunofluorescence of GFP-Zw10/mCherry-Tubulin expressing cells after
705 depletion of Spc105R. At day 4 of RNAi, cells were fixed and stained with anti-GFP (green) and
706 anti-Spc105R antibodies (red), DNA was counterstained with DAPI. **E.** Immunofluorescence
707 of S2 cells after depletion of Zw10. At day 4 of RNAi, cells were fixed and stained with anti-
708 Zw10 (green), anti-Spc105R (red) and anti-tubulin (grey) antibodies, DNA was counterstained
709 with DAPI. Scale bar= 2 µm. **F.** Quantification of E. showing the total Spc105R kinetochore
710 intensity per cell. Spc105R fluorescence intensity at kinetochores was measured for each cell

711 and then normalized within one experiment allowing pooling of the measurements for at
712 least 3 experiments per condition. Mean +/- SEM (n>90 cells), Student t-test (n.s.: non-
713 significant) **G.** Immunofluorescence of S2 cells after depletion of Zw10. At day 4 of RNAi, cells
714 were fixed and stained with anti-Ndc80 (green), anti-Spc105R (red) and anti-tubulin (grey)
715 antibodies, DNA was counterstained with DAPI. Scale bar= 2 µm. **H.** Quantification of G.
716 showing the total Ndc80 kinetochore intensity per cell. Ndc80 fluorescence intensity at
717 kinetochores was measured for each cell and then normalized within one experiment
718 allowing pooling of the measurements for at least 3 experiments per condition. Mean +/- SEM
719 (n>90 cells), Student t-test (n.s.: non-significant).

720

721

722

723

724

725

726 Online supplemental materials include 6 figures and 10 videos. Fig. S1 shows GFP-CENP-A
727 FRAP in early G1 and SNAP-CENP-A centromeric loading outside mitosis. Fig. S2 shows SAC
728 activity and kinetochore components recruitment in CAL1-overexpressing cells. Fig. S3 shows
729 qPCR results for RNAi efficiency in SNAP-CENP-A cells, SNAP-CENP-A and SNAP-CAL1 quench-
730 chase-pulse experiments in different RNAi and drug treatments. Fig. S4 shows yeast two
731 hybrid with CAL1 and Zw10 fragments, pulldown assay between GST-Zw10 and CENP-A and
732 localization of the GFP-tagged RZZ-proteins during cell cycle. Fig. S5 shows SNAP-CAL1
733 quench-chase-pulse experiment in Zw10-depleted cells, centromeric SNAP-CENP-A stability
734 assay and GFP-CENP-A FRAP during mitosis in Zw10-depleted cells. Fig. S6 shows qPCR results
735 for RNAi efficiency in GFP-Zw10 cells, GFP-Zw10 localization in CAL1, Bub1 and Mis12-
736 depleted cells, Mis12 and BubR1 localization in Zw10-depleted cells.

737

738 **Supplemental figures legends**

739 **Figure S1 related to fig. 1-2.**

740 **A.** FRAP of GFP-CENP-A in G1 phase. Cells expressing GFP-CENP-A and mCherry-Tubulin were
741 followed through mitosis, GFP-CENP-A signal was partially bleached in early G1 and cells were
742 further imaged for > 2 h. Time lapse: 6 min. Scale bar: 2 µm. **B.** Quantification of A. The total
743 GFP-CENP-A centromeric signal of 6 cells is shown as mean +/- SEM. **C.** Quantification of cells
744 showing SNAP-CENP-A signal at centromeres in control and CAL1-overexpressing cells after 4
745 h MG132 treatment. CAL1-V5 expression was induced for 24 h. The cells were then incubated
746 for 2 h with MG132 to arrest cells in mitosis prior to SNAP-CENP-A block. A 4-h chase was
747 performed in presence of MG132 to allow synthesis and incorporation of new SNAP-CENP-A
748 into centromeres before incubation with SNAP-Si647 and fixation. **C.** Immunofluorescence of

749 SNAP-CENP-A in control and CAL1 overexpressing cells. CAL1-V5 expression was induced for
750 24 h. The cells were then incubated with SNAP-Block, washed and resuspended in conditional
751 medium containing SNAP-640 dye. After 20 h, the cells were washed 3 times before fixation
752 and immunostaining with an anti-CENP-A antibody (green). Cells were also taken after block,
753 stained with 0.5 µM SNAP-640 dye for 15 min to check the efficiency of the block. DNA was
754 counterstained with DAPI. Scale bar= 2 µm. **D.** Quantification of C. showing the percentage of
755 cells positive for centromeric SNAP-CENP-A staining. **E.** Quantification of B. showing the total
756 SNAP-CENP-A centromeric intensity per nucleus as % of control. All graphs show Mean +/-
757 SEM of 3 experiments (n>300 cells), Student t-test (n.s.: non-significant; *: $p<0.05$; **:
758 $p<0.01$).

759

760 **Figure S2 related to fig. 2**

761 **A.** Mitotic phenotypes of H2B-GFP/mCherry-Tubulin expressing cells with or without
762 concomitant overexpression of CAL1. CAL1-V5 expression was induced for 24 h with 100 µM
763 $CuSO_4$ then the cells were imaged for 16 h. Cells were scored for the accuracy of mitosis:
764 normal or defective (presence of lagging chromosomes in anaphase, formation of tripolar
765 spindles). Mean +/- SEM n > 200 cells. Student t-test (*n.s.*: non-significant). **B.** Amount of
766 kinetochore proteins recruited during mitosis in presence or absence of CAL1 overexpression.
767 CAL1-V5 expression was induced for 24 h in GFP-CENP-A/mCherry-Tubulin cells. Cells were
768 then fixed and stained with anti-CENP-C (upper panel, red), anti-Spc105R (middle panel, red)
769 or anti-BubR1 antibody (lower panel, red). DNA was counterstained with DAPI. Scale bar= 2
770 µm. Kinetochore signal intensity of the indicated proteins is shown as % of control. Only
771 prometaphase cells were analyzed. Mean +/- SEM of 3 experiments (n > 300 cells). Student t-

772 test (*n.s.*: non-significant). **C.** Stills from time-lapse imaging experiments showing GFP-CENP-
773 A/mCherry-Tubulin cells with or without CAL1 overexpression imaged immediately after
774 addition of 1 µM Taxol and after 5 h. CAL1-V5 expression was induced for 24 h. Then 1 µM
775 taxol was added and the cells were imaged for 16 h. Scale bar= 2 µm. **D.** Quantification of C.
776 showing the percentage of cells that arrest (arrest) in response to Taxol treatment or arrest
777 and restart (finish).

778

779 **Figure S3 related to fig. 4**

780 **A.** qPCR results showing mRNA levels after indicated knockdown in SNAP-CENP-A cells as
781 percent of control. **B.** Immunofluorescence of SNAP-CENP-A expressing cells after MG132 or
782 Nocodazole treatment. A Quench-Chase-Pulse experiment was performed to stain newly
783 synthesized SNAP-CENP-A molecules. The 24 h chase was performed in presence or absence
784 of the indicated drug. Cells were stained with an anti-S10-phospho-H3 antibody to identify
785 mitotic cells. DNA was counterstained with DAPI. Scale bar= 2 µm. **C.** Quantification of B.
786 showing the SNAP-CENP-A centromeric intensity as % of control. Only Phospho-H3 positive
787 cells were analyzed. Mean+/- SEM of 3 experiments (n>300 cells), Student t-test (n.s= non-
788 significant). **D.** Quantification showing the total SNAP-CAL1 centromeric intensity per nucleus
789 as % of control after knockdown of the indicated proteins. Mean+/- SEM of 3 experiments
790 (n>300 cells), Student t-test (**: p<0.01; n.s.: non-significant).

791

792 **Figure S4 related to fig. 5**

793 **A.** Yeast two hybrid interaction tests. Blue color reflects the interaction between the 2
794 proteins tested. **B.** Scheme showing CAL1 functional domains and its binding to its known
795 partners. BD: binding domain. **C.** ***Left panel.*** Coomassie showing purified His-Sumo-CENP-A.
796 ***Right panel.*** Pulldown assay between GST or GST-Zw10 with His-Sumo-CENP-A. **D-F.**
797 Localization of GFP-Zw10 (**D**), GFP-Zwilch (**E**), GFP-ROD (**F**) during cell cycle. Cells expressing
798 each GFP-RZZ component concomitant with mCherry-Tubulin were fixed and stained with
799 anti-GFP (green) and anti-CENP-A (red) antibodies, DNA was counterstained with DAPI. Scale
800 bar= 2 µm.

801

802 **Figure S5 related to fig. 5**

803 **A.** Immunofluorescence of SNAP-CAL1 expressing cells after Zw10 depletion. After 72 h dsRNA
804 treatment, a Quench-Chase-Pulse experiment (scheme in Fig. 1H) was performed to stain
805 newly synthesized SNAP-CAL1 molecules. DNA was counterstained with DAPI. Scale bar= 2
806 µm. **B.** Quantification of A. showing the total SNAP-CAL1 centromeric intensity per nucleus as
807 % of control. Mean +/- SEM of 3 experiments (n>300 cells), Student t-test (**: p<0.01). **C.**
808 Immunofluorescence of SNAP-CENP-A expressing cells after Zw10 depletion. After 72 h dsRNA
809 treatment, cells were incubated with TMR-Star (P) to stain existing SNAP-CENP-A molecules,
810 washed and put back in culture (t0). After 24 h chase, cells were fixed (t24). Note that no
811 SNAP-Block was performed for this experiment. DNA was counterstained with DAPI. Scale
812 bar= 2 µm. **D.** Quantification of C. showing the total SNAP-CENP-A centromeric intensity per
813 nucleus as % of t0. Mean +/- SEM of 3 experiments (n>300 cells), Student t-test (n.s= non-
814 significant). **E.** FRAP of GFP-CENP-A in mitosis after Zw10 depletion. After 72 h dsRNA
815 treatment, GFP-CENP-A signal was partially (about 50-60 %) bleached in prophase and cells

816 were imaged until telophase. Time lapse: 90 s. Scale bar= 2 µm. **F.** Quantification of E. The
817 total GFP-CENP-A centromeric signal of at least 8 cells is displayed as mean +/- SEM.

818

819 **Figure S6 related to fig. 6-7**

820 **A.** qPCR results showing mRNA levels after indicated knockdown in GFP-Zw10 cells as percent
821 of control. **B-D.** Immunofluorescence of GFP-Zw10/mCherry-Tubulin expressing cells after
822 depletion of CAL1 (**B**), Bub1 (**C**) or Mis12 (**D**). After 96 h dsRNA treatment, cells were fixed and
823 stained with anti-GFP (green) and anti-CENP-A (B) or Scp105R (C-D)(red) antibodies, DNA was
824 counterstained with DAPI. Scale bar= 2 µm. **E.** Immunofluorescence of S2 cells after depletion
825 of Zw10. At day 4 of RNAi, cells were fixed and stained with anti-Mis12 (green), anti-Spc105R
826 (red) and anti-tubulin (grey) antibodies, DNA was counterstained with DAPI. Scale bar= 2 µm.
827 **F.** Quantification of E. showing the total Mis12 kinetochore intensity per mitotic cell. Mis12
828 fluorescence intensity at kinetochores was measured for each cell and then normalized within
829 one experiment allowing pooling of the measurements for at least 3 experiments per
830 condition. Mean +/- SEM (n>90 cells), Student t-test (n.s.: non-significant). **G.**
831 Immunofluorescence of S2 cells after depletion of Zw10. At day 4 of RNAi, cells were fixed
832 and stained with anti-BubR1 (green) and anti-tubulin (grey) antibodies, DNA was
833 counterstained with DAPI. Scale bar= 2 µm. **H.** Quantification of G. showing the total BubR1
834 kinetochore intensity per mitotic cell. BubR1 fluorescence intensity at kinetochores was
835 measured for each cell and then normalized within one experiment allowing pooling of the
836 measurements for at least 3 experiments per condition. Mean +/- SEM (n>90 cells), Student
837 t-test (n.s.: non-significant).

838 **<u>Supplemental Videos.</u>**

839 **Video 1 (related to Figure 2D).**

840 SNAP-CENP-A/mCherry-tubulin expressing cells containing inducible CAL1-V5. No CAL1-V5
841 induction. SNAP-CENP-A molecules were quenched before addition of 0.5 µM SNAP-640 dye.
842 Imaging was performed for 16 h on a Deltavision microscope (60X, Bin 2), at 25°C. Time lapse
843 15 min. Scale bar= 5 µm.

844

845 **Video 2 (related to Figure 2D):**

846 SNAP-CENP-A/mCherry-tubulin expressing cells containing inducible CAL1-V5. CAL1-V5
847 expression was induced for 24 h with 100 µM $CuSO_4$. SNAP-CENP-A molecules were quenched
848 before addition of 0.5 µM SNAP-640 dye. Imaging was performed for 16 h on a Deltavision
849 microscope (60X, Bin 2), at 25°C. Time lapse 15 min. Scale bar= 5 µm.

850

851 **Video 3 (related to Figure 2G):**

852 H2B-GFP/mCherry-tubulin expressing cells containing inducible CAL1-V5. No CAL1-V5
853 induction. Imaging was performed for 16 h on a Deltavision microscope (60X, Bin 2), at 25°C.
854 Time lapse 3 min. Scale bar= 5 µm.

855

856 **Video 4 (related to Figure 2G):**

857 H2B-GFP/mCherry-tubulin expressing cells containing inducible CAL1-V5. CAL1-V5 expression
858 was induced for 24 h prior to imaging with 100 µM $CuSO_4$. Imaging was performed for 16 h
859 on a Deltavision microscope (60X, Bin 2), at 25°C. Time lapse 3 min. Scale bar= 5 µm.

860

861 **Video 5 (related to Figure 3C):**

862 GFP-CENP-A/mCherry-Tubulin expressing cells after Ctrl dsRNA treatment (72 h). Imaging was
863 performed for 16 h on a Deltavision microscope (40X, Bin 2), at 25°C. Time lapse 3 min. Scale
864 bar= 5 µm.
865

866 **Video 6 (related to Figure 3C):**

867 GFP-CENP-A/mCherry-Tubulin expressing cells after CENP-A dsRNA treatment (72 h). Imaging
868 was performed for 16 h on a Deltavision microscope (40X, Bin 2), at 25°C. Time lapse 3 min.
869 Scale bar= 5 µm.
870

871 **Video 7 (related to Figure 3I):**

872 CENP-A-GFP/mCherry-tubulin expressing cells. Visible CENP-A-GFP results from leaky
873 metallothionein promoter. Imaging was performed for 16 h on a Deltavision microscope (40X,
874 Bin 2), at 25 °C. Time lapse 3 min. Scale bar= 5 µm.
875

876 **Video 8 (related to Figure 3I):**

877 CENP-A-GFP/mCherry-tubulin expressing cells. CENP-A-GFP expression was induced for 2 h
878 with 10 µM $CuSO_4$ then washed 3 times before being placed in Ibidi chamber. Imaging was
879 performed for 16 h on a Deltavision microscope (40X, Bin 2), at 25°C. Time lapse 3 min. Scale
880 bar= 5 µm.

881

882 **Video 9 (related to Figure 5E):**

883 H2B-GFP/mCherry-tubulin expressing cells after Ctrl dsRNA treatment (72 h). Imaging was
884 performed for 16 h on a Deltavision microscope (60X, Bin 2), at 25°C. Time lapse 3 min. Scale
885 bar= 5 µm.

886

887 **Video 10 (related Figure 5E):**

888 H2B-GFP/mCherry-tubulin expressing cells after Zw10 dsRNA treatment (72 h). Imaging was
889 performed for 16 h on a Deltavision microscope (60X, Bin 2), at 25°C. Time lapse 3 min. Scale
890 bar= 5 µm.

891

892 **References**

893 1. Joglekar AP, Kukreja AA. How Kinetochore Architecture Shapes the Mechanisms of Its
894 Function. Curr Biol. 2017;27(16):R816-R24.
895 2. Musacchio A, Desai A. A Molecular View of Kinetochore Assembly and Function. Biology
896 (Basel). 2017;6(1).
897 3. Kapanidou M, Curtis NL, Bolanos-Garcia VM. Cdc20: At the Crossroads between Chromosome
898 Segregation and Mitotic Exit. Trends Biochem Sci. 2017;42(3):193-205.
899 4. Musacchio A. The Molecular Biology of Spindle Assembly Checkpoint Signaling Dynamics. Curr
900 Biol. 2015;25(20):R1002-18.
901 5. Jansen LE, Black BE, Foltz DR, Cleveland DW. Propagation of centromeric chromatin requires
902 exit from mitosis. J Cell Biol. 2007;176(6):795-805.
903 6. Takayama Y, Sato H, Saitoh S, Ogiyama Y, Masuda F, Takahashi K. Biphasic incorporation of
904 centromeric histone CENP-A in fission yeast. Mol Biol Cell. 2008;19(2):682-90.
905 7. Shukla M, Tong P, White SA, Singh PP, Reid AM, Catania S, et al. Centromere DNA Destabilizes
906 H3 Nucleosomes to Promote CENP-A Deposition during the Cell Cycle. Curr Biol. 2018;28(24):3924-36
907 e4.
908 8. Lermontova I, Schubert V, Fuchs J, Klatte S, Macas J, Schubert I. Loading of Arabidopsis
909 centromeric histone CENH3 occurs mainly during G2 and requires the presence of the histone fold
910 domain. Plant Cell. 2006;18(10):2443-51.
911 9. Schuh M, Lehner CF, Heidmann S. Incorporation of Drosophila CID/CENP-A and CENP-C into
912 centromeres during early embryonic anaphase. Curr Biol. 2007;17(3):237-43.
913 10. Mellone BG, Grive KJ, Shteyn V, Bowers SR, Oderberg I, Karpen GH. Assembly of Drosophila
914 centromeric chromatin proteins during mitosis. PLoS Genet. 2011;7(5):e1002068.
915 11. Dunleavy EM, Beier NL, Gorgescu W, Tang J, Costes SV, Karpen GH. The cell cycle timing of
916 centromeric chromatin assembly in Drosophila meiosis is distinct from mitosis yet requires CAL1 and
917 CENP-C. PLoS Biol. 2012;10(12):e1001460.
918 12. Lidsky PV, Sprenger F, Lehner CF. Distinct modes of centromere protein dynamics during cell
919 cycle progression in Drosophila S2R+ cells. J Cell Sci. 2013;126(Pt 20):4782-93.
920 13. Chen CC, Mellone BG. Chromatin assembly: Journey to the CENter of the chromosome. J Cell
921 Biol. 2016;214(1):13-24.

922 14. Foltz DR, Jansen LE, Bailey AO, Yates JR, 3rd, Bassett EA, Wood S, et al. Centromere-specific
923 assembly of CENP-a nucleosomes is mediated by HJURP. Cell. 2009;137(3):472-84.
924 15. Camahort R, Li B, Florens L, Swanson SK, Washburn MP, Gerton JL. Scm3 is essential to recruit
925 the histone h3 variant cse4 to centromeres and to maintain a functional kinetochore. Mol Cell.
926 2007;26(6):853-65.
927 16. Dunleavy EM, Roche D, Tagami H, Lacoste N, Ray-Gallet D, Nakamura Y, et al. HJURP is a cell-
928 cycle-dependent maintenance and deposition factor of CENP-A at centromeres. Cell. 2009;137(3):485-
929 97.
930 17. Mizuguchi G, Xiao H, Wisniewski J, Smith MM, Wu C. Nonhistone Scm3 and histones CenH3-
931 H4 assemble the core of centromere-specific nucleosomes. Cell. 2007;129(6):1153-64.
932 18. Chen CC, Dechassa ML, Bettini E, Ledoux MB, Belisario C, Heun P, et al. CAL1 is the Drosophila
933 CENP-A assembly factor. J Cell Biol. 2014;204(3):313-29.
934 19. Stoler S, Rogers K, Weitze S, Morey L, Fitzgerald-Hayes M, Baker RE. Scm3, an essential
935 Saccharomyces cerevisiae centromere protein required for G2/M progression and Cse4 localization.
936 Proc Natl Acad Sci U S A. 2007;104(25):10571-6.
937 20. Erhardt S, Mellone BG, Betts CM, Zhang W, Karpen GH, Straight AF. Genome-wide analysis
938 reveals a cell cycle-dependent mechanism controlling centromere propagation. J Cell Biol.
939 2008;183(5):805-18.
940 21. Collins KA, Furuyama S, Biggins S. Proteolysis contributes to the exclusive centromere
941 localization of the yeast Cse4/CENP-A histone H3 variant. Curr Biol. 2004;14(21):1968-72.
942 22. Hewawasam G, Shivaraju M, Mattingly M, Venkatesh S, Martin-Brown S, Florens L, et al. Psh1
943 is an E3 ubiquitin ligase that targets the centromeric histone variant Cse4. Mol Cell. 2010;40(3):444-
944 54.
945 23. Moreno-Moreno O, Torras-Llort M, Azorin F. Proteolysis restricts localization of CID, the
946 centromere-specific histone H3 variant of Drosophila, to centromeres. Nucleic Acids Res.
947 2006;34(21):6247-55.
948 24. Heun P, Erhardt S, Blower MD, Weiss S, Skora AD, Karpen GH. Mislocalization of the Drosophila
949 centromere-specific histone CID promotes formation of functional ectopic kinetochores. Dev Cell.
950 2006;10(3):303-15.
951 25. Olszak AM, van Essen D, Pereira AJ, Diehl S, Manke T, Maiato H, et al. Heterochromatin
952 boundaries are hotspots for de novo kinetochore formation. Nat Cell Biol. 2011;13(7):799-808.
953 26. Muller S, Almouzni G. Chromatin dynamics during the cell cycle at centromeres. Nat Rev
954 Genet. 2017;18(3):192-208.
955 27. Westermann S, Schleiffer A. Family matters: structural and functional conservation of
956 centromere-associated proteins from yeast to humans. Trends Cell Biol. 2013;23(6):260-9.
957 28. Przewloka MR, Venkei Z, Bolanos-Garcia VM, Debski J, Dadlez M, Glover DM. CENP-C Is a
958 Structural Platform for Kinetochore Assembly. Curr Biol. 2011;21(5):399-405.
959 29. Bade D, Pauleau AL, Wendler A, Erhardt S. The E3 ligase CUL3/RDX controls centromere
960 maintenance by ubiquitylating and stabilizing CENP-A in a CAL1-dependent manner. Dev Cell.
961 2014;28(5):508-19.
962 30. Schittenhelm RB, Althoff F, Heidmann S, Lehner CF. Detrimental incorporation of excess Cenp-
963 A/Cid and Cenp-C into Drosophila centromeres is prevented by limiting amounts of the bridging factor
964 Cal1. J Cell Sci. 2010;123(Pt 21):3768-79.
965 31. Butkevich AN, Belov VN, Kolmakov K, Sokolov VV, Shojaei H, Sidenstein SC, et al. Hydroxylated
966 Fluorescent Dyes for Live-Cell Labeling: Synthesis, Spectra and Super-Resolution STED. Chemistry.
967 2017;23(50):12114-9.
968 32. Blower MD, Karpen GH. The role of Drosophila CID in kinetochore formation, cell-cycle
969 progression and heterochromatin interactions. Nat Cell Biol. 2001;3(8):730-9.
970 33. Blower MD, Daigle T, Kaufman T, Karpen GH. Drosophila CENP-A mutations cause a BubR1-
971 dependent early mitotic delay without normal localization of kinetochore components. PLoS Genet.
972 2006;2(7):e110.

973 34. Orr B, Bousbaa H, Sunkel CE. Mad2-independent spindle assembly checkpoint activation and
974 controlled metaphase-anaphase transition in Drosophila S2 cells. Mol Biol Cell. 2007;18(3):850-63.
975 35. Rahmani Z, Gagou ME, Lefebvre C, Emre D, Karess RE. Separating the spindle, checkpoint, and
976 timer functions of BubR1. J Cell Biol. 2009;187(5):597-605.
977 36. Lince-Faria M, Maffini S, Orr B, Ding Y, Claudia F, Sunkel CE, et al. Spatiotemporal control of
978 mitosis by the conserved spindle matrix protein Megator. J Cell Biol. 2009;184(5):647-57.
979 37. Feijao T, Afonso O, Maia AF, Sunkel CE. Stability of kinetochore-microtubule attachment and
980 the role of different KMN network components in Drosophila. Cytoskeleton (Hoboken).
981 2013;70(10):661-75.
982 38. Griffis ER, Stuurman N, Vale RD. Spindly, a novel protein essential for silencing the spindle
983 assembly checkpoint, recruits dynein to the kinetochore. J Cell Biol. 2007;177(6):1005-15.
984 39. Huang JY, Raff JW. The dynamic localisation of the Drosophila APC/C: evidence for the
985 existence of multiple complexes that perform distinct functions and are differentially localised. J Cell
986 Sci. 2002;115(Pt 14):2847-56.
987 40. Scaerou F, Starr DA, Piano F, Papoulas O, Karess RE, Goldberg ML. The ZW10 and Rough Deal
988 checkpoint proteins function together in a large, evolutionarily conserved complex targeted to the
989 kinetochore. J Cell Sci. 2001;114(Pt 17):3103-14.
990 41. Williams BC, Karr TL, Montgomery JM, Goldberg ML. The Drosophila l(1)zw10 gene product,
991 required for accurate mitotic chromosome segregation, is redistributed at anaphase onset. J Cell Biol.
992 1992;118(4):759-73.
993 42. Williams BC, Goldberg ML. Determinants of Drosophila zw10 protein localization and function.
994 J Cell Sci. 1994;107 (Pt 4):785-98.
995 43. Williams BC, Gatti M, Goldberg ML. Bipolar spindle attachments affect redistributions of
996 ZW10, a Drosophila centromere/kinetochore component required for accurate chromosome
997 segregation. J Cell Biol. 1996;134(5):1127-40.
998 44. Defachelles L, Raich N, Terracol R, Baudin X, Williams B, Goldberg M, et al. RZZ and Mad1
999 dynamics in Drosophila mitosis. Chromosome Res. 2015;23(2):333-42.
1000 45. Starr DA, Williams BC, Hays TS, Goldberg ML. ZW10 helps recruit dynactin and dynein to the
1001 kinetochore. J Cell Biol. 1998;142(3):763-74.
1002 46. Wojcik E, Basto R, Serr M, Scaerou F, Karess R, Hays T. Kinetochore dynein: its dynamics and
1003 role in the transport of the Rough deal checkpoint protein. Nat Cell Biol. 2001;3(11):1001-7.
1004 47. Gassmann R, Essex A, Hu JS, Maddox PS, Motegi F, Sugimoto A, et al. A new mechanism
1005 controlling kinetochore-microtubule interactions revealed by comparison of two dynein-targeting
1006 components: SPDL-1 and the Rod/Zwilch/Zw10 complex. Genes Dev. 2008;22(17):2385-99.
1007 48. Buffin E, Lefebvre C, Huang J, Gagou ME, Karess RE. Recruitment of Mad2 to the kinetochore
1008 requires the Rod/Zw10 complex. Curr Biol. 2005;15(9):856-61.
1009 49. Scaerou F, Aguilera I, Saunders R, Kane N, Blottiere L, Karess R. The rough deal protein is a
1010 new kinetochore component required for accurate chromosome segregation in Drosophila. J Cell Sci.
1011 1999;112 (Pt 21):3757-68.
1012 50. Basto R, Gomes R, Karess RE. Rough deal and Zw10 are required for the metaphase checkpoint
1013 in Drosophila. Nat Cell Biol. 2000;2(12):939-43.
1014 51. Basto R, Scaerou F, Mische S, Wojcik E, Lefebvre C, Gomes R, et al. In vivo dynamics of the
1015 rough deal checkpoint protein during Drosophila mitosis. Curr Biol. 2004;14(1):56-61.
1016 52. Williams BC, Li Z, Liu S, Williams EV, Leung G, Yen TJ, et al. Zwilch, a new component of the
1017 ZW10/ROD complex required for kinetochore functions. Mol Biol Cell. 2003;14(4):1379-91.
1018 53. Karess RE, Glover DM. rough deal: a gene required for proper mitotic segregation in
1019 Drosophila. J Cell Biol. 1989;109(6 Pt 1):2951-61.
1020 54. Defachelles L, Hainline SG, Menant A, Lee LA, Karess RE. A maternal effect rough deal mutation
1021 suggests that multiple pathways regulate Drosophila RZZ kinetochore recruitment. J Cell Sci.
1022 2015;128(15):2952.

1023 55. Wainman A, Giansanti MG, Goldberg ML, Gatti M. The Drosophila RZZ complex - roles in
1024 membrane trafficking and cytokinesis. J Cell Sci. 2012;125(Pt 17):4014-25.
1025 56. Przewloka MR, Zhang W, Costa P, Archambault V, D'Avino PP, Lilley KS, et al. Molecular
1026 analysis of core kinetochore composition and assembly in Drosophila melanogaster. PLoS One.
1027 2007;2(5):e478.
1028 57. Starr DA, Saffery R, Li Z, Simpson AE, Choo KH, Yen TJ, et al. HZwint-1, a novel human
1029 kinetochore component that interacts with HZW10. J Cell Sci. 2000;113 (Pt 11):1939-50.
1030 58. Kops GJ, Kim Y, Weaver BA, Mao Y, McLeod I, Yates JR, 3rd, et al. ZW10 links mitotic checkpoint
1031 signaling to the structural kinetochore. J Cell Biol. 2005;169(1):49-60.
1032 59. Caldas GV, Lynch TR, Anderson R, Afreen S, Varma D, DeLuca JG. The RZZ complex requires
1033 the N-terminus of KNL1 to mediate optimal Mad1 kinetochore localization in human cells. Open Biol.
1034 2015;5(11).
1035 60. Kasuboski JM, Bader JR, Vaughan PS, Tauhata SB, Winding M, Morrissey MA, et al. Zwint-1 is
1036 a novel Aurora B substrate required for the assembly of a dynein-binding platform on kinetochores.
1037 Mol Biol Cell. 2011;22(18):3318-30.
1038 61. Zhang G, Lischetti T, Hayward DG, Nilsson J. Distinct domains in Bub1 localize RZZ and BubR1
1039 to kinetochores to regulate the checkpoint. Nat Commun. 2015;6:7162.
1040 62. Schittenhelm RB, Chaleckis R, Lehner CF. Intrakinetochore localization and essential functional
1041 domains of Drosophila Spc105. EMBO J. 2009;28(16):2374-86.
1042 63. Orr B, Sunkel CE. Drosophila CENP-C is essential for centromere identity. Chromosoma.
1043 2010;120(1):83-96.
1044 64. Basu J, Logarinho E, Herrmann S, Bousbaa H, Li Z, Chan GK, et al. Localization of the Drosophila
1045 checkpoint control protein Bub3 to the kinetochore requires Bub1 but not Zw10 or Rod. Chromosoma.
1046 1998;107(6-7):376-85.
1047 65. Lacoste N, Woolfe A, Tachiwana H, Garea AV, Barth T, Cantaloube S, et al. Mislocalization of
1048 the centromeric histone variant CenH3/CENP-A in human cells depends on the chaperone DAXX. Mol
1049 Cell. 2014;53(4):631-44.
1050 66. Meraldi P, Draviam VM, Sorger PK. Timing and checkpoints in the regulation of mitotic
1051 progression. Dev Cell. 2004;7(1):45-60.
1052 67. Buffin E, Emre D, Karess RE. Flies without a spindle checkpoint. Nat Cell Biol. 2007;9(5):565-
1053 72.
1054 68. Emre D, Terracol R, Poncet A, Rahmani Z, Karess RE. A mitotic role for Mad1 beyond the
1055 spindle checkpoint. J Cell Sci. 2011;124(Pt 10):1664-71.
1056 69. Li J, Dang N, Wood DJ, Huang JY. The kinetochore-dependent and -independent formation of
1057 the CDC20-MAD2 complex and its functions in HeLa cells. Sci Rep. 2017;7:41072.
1058 70. Sacristan C, Ahmad MUD, Keller J, Fermie J, Groenewold V, Tromer E, et al. Dynamic
1059 kinetochore size regulation promotes microtubule capture and chromosome biorientation in mitosis.
1060 Nat Cell Biol. 2018;20(7):800-10.
1061 71. Pereira C, Reis RM, Gama JB, Celestino R, Cheerambathur DK, Carvalho AX, et al. Self-Assembly
1062 of the RZZ Complex into Filaments Drives Kinetochore Expansion in the Absence of Microtubule
1063 Attachment. Curr Biol. 2018;28(21):3408-21 e8.
1064 72. Rodriguez-Rodriguez JA, Lewis C, McKinley KL, Sikirzhytski V, Corona J, Maciejowski J, et al.
1065 Distinct Roles of RZZ and Bub1-KNL1 in Mitotic Checkpoint Signaling and Kinetochore Expansion. Curr
1066 Biol. 2018;28(21):3422-9 e5.
1067 73. London N, Biggins S. Mad1 kinetochore recruitment by Mps1-mediated phosphorylation of
1068 Bub1 signals the spindle checkpoint. Genes Dev. 2014;28(2):140-52.
1069 74. Moyle MW, Kim T, Hattersley N, Espeut J, Cheerambathur DK, Oegema K, et al. A Bub1-Mad1
1070 interaction targets the Mad1-Mad2 complex to unattached kinetochores to initiate the spindle
1071 checkpoint. J Cell Biol. 2014;204(5):647-57.
1072 75. Silio V, McAinsh AD, Millar JB. KNL1-Bubs and RZZ Provide Two Separable Pathways for
1073 Checkpoint Activation at Human Kinetochores. Dev Cell. 2015;35(5):600-13.

1074 76. Varma D, Wan X, Cheerambathur D, Gassmann R, Suzuki A, Lawrimore J, et al. Spindle
1075 assembly checkpoint proteins are positioned close to core microtubule attachment sites at
1076 kinetochores. J Cell Biol. 2013;202(5):735-46.
1077 77. Petsalaki E, Dandoulaki M, Zachos G. The ESCRT protein Chmp4c regulates mitotic spindle
1078 checkpoint signaling. J Cell Biol. 2018;217(3):861-76.
1079 78. Schittenhelm RB, Heeger S, Althoff F, Walter A, Heidmann S, Mechtler K, et al. Spatial
1080 organization of a ubiquitous eukaryotic kinetochore protein network in Drosophila chromosomes.
1081 Chromosoma. 2007;116(4):385-402.
1082 79. Ahmad K, Henikoff S. Centromeres are specialized replication domains in heterochromatin. J
1083 Cell Biol. 2001;153(1):101-10.
1084 80. Mathew V, Pauleau AL, Steffen N, Bergner A, Becker PB, Erhardt S. The histone-fold protein
1085 CHRAC14 influences chromatin composition in response to DNA damage. Cell Rep. 2014;7(2):321-30.
1086 81. Rothbauer U, Zolghadr K, Muyldermans S, Schepers A, Cardoso MC, Leonhardt H. A versatile
1087 nanotrap for biochemical and functional studies with fluorescent fusion proteins. Mol Cell Proteomics.
1088 2008;7(2):282-9.
1089 82. Venkei Z, Przewloka MR, Glover DM. Drosophila Mis12 complex acts as a single functional unit
1090 essential for anaphase chromosome movement and a robust spindle assembly checkpoint. Genetics.
1091 2011;187(1):131-40.
1092 83. Schramm C, Elliott S, Shevchenko A, Schiebel E. The Bbp1p-Mps2p complex connects the SPB
1093 to the nuclear envelope and is essential for SPB duplication. EMBO J. 2000;19(3):421-33.

1094

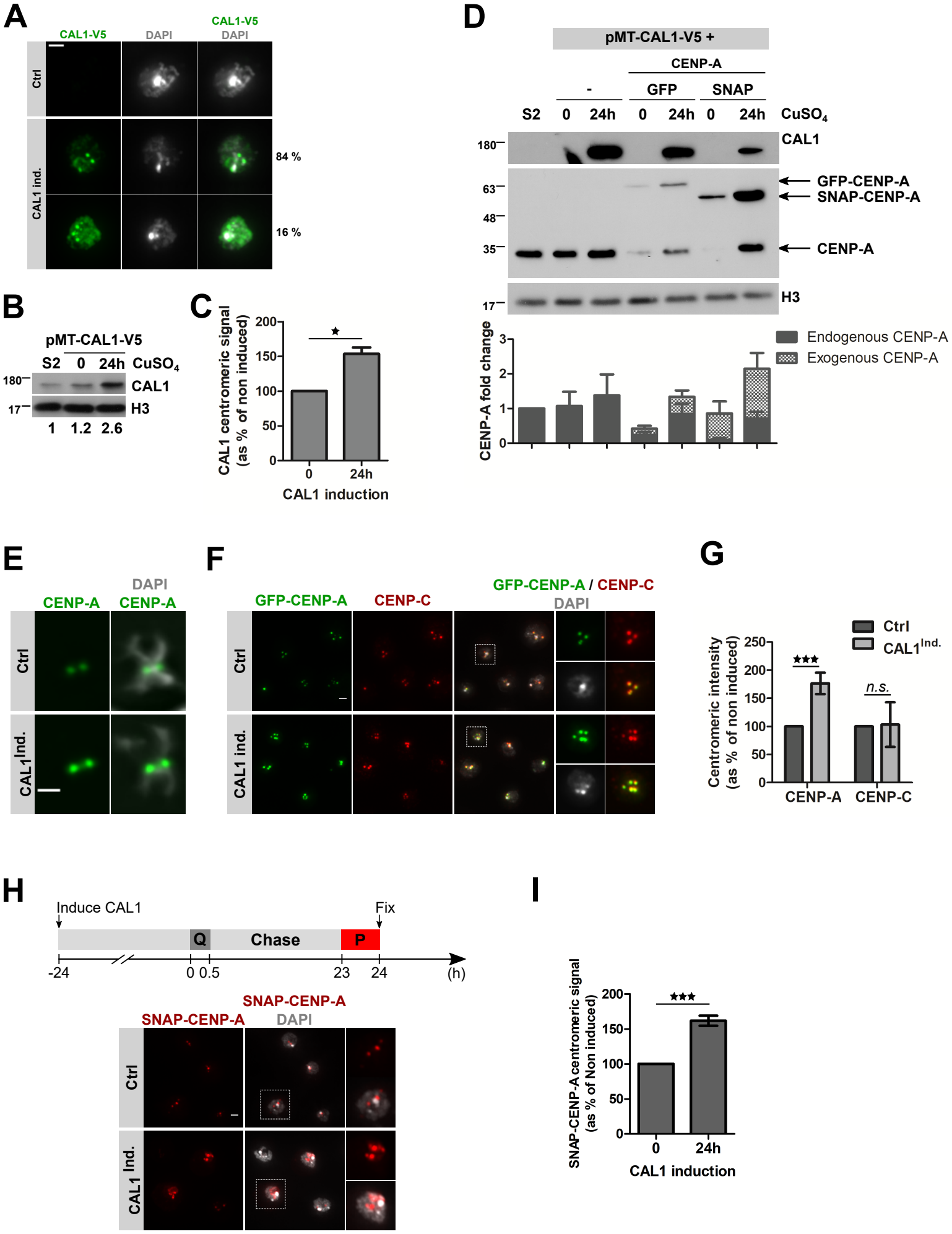
A
CAL1-V5
DAPI
CAL1-V5
DAPI
Ctrl
CAL1 ind.
84 %
16 %
B
pMT-CAL1-V5
S2
0
24h
CuSO4
180
17
CAL1
H3
1
1.2
2.6
C
CAL1 centromeric signal (as % of non induced)
200
150
100
50
0
0
24h
CAL1 induction
D
pMT-CAL1-V5 +
CENP-A
-
GFP
SNAP
S2
0
24h
0
24h
0
24h
CuSO4
180
63
48
35
17
CAL1
GFP-CENP-A
SNAP-CENP-A
CENP-A
H3
CENP-A fold change
3
2
1
0
Endogenous CENP-A
Exogenous CENP-A
E
DAPI
CENP-A
CENP-A
Ctrl
CAL1 Ind.
F
GFP-CENP-A
CENP-C
GFP-CENP-A / CENP-C
DAPI
Ctrl
CAL1 ind.
G
Ctrl
CAL1 Ind.
Centromeric intensity (as % of non induced)
250
200
150
100
50
0
***
n.s.
CENP-A
CENP-C
H
Induce CAL1
Fix
Q
Chase
P
-24
0
0.5
23
24
(h)
SNAP-CENP-A
SNAP-CENP-A
DAPI
Ctrl
CAL1 Ind.
I
SNAP-CENP-A centromeric signal (as % of Non induced)
200
150
100
50
0
***
0
24h
CAL1 induction

Fig.1

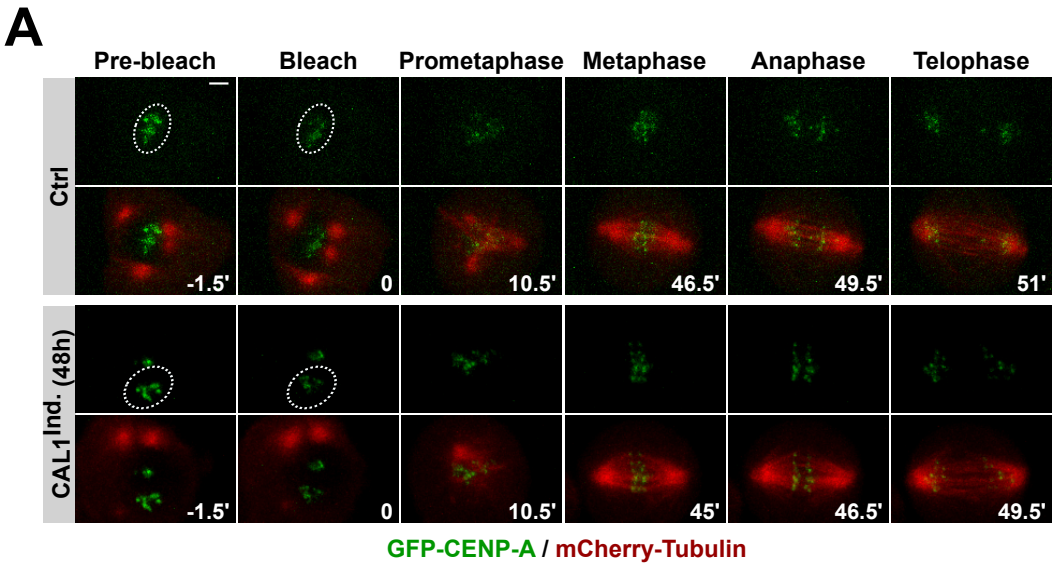

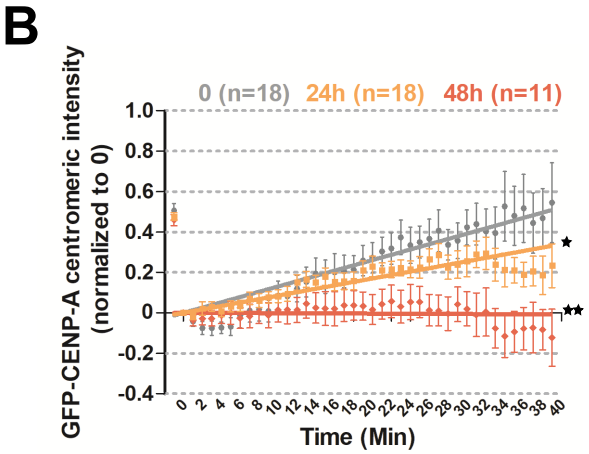

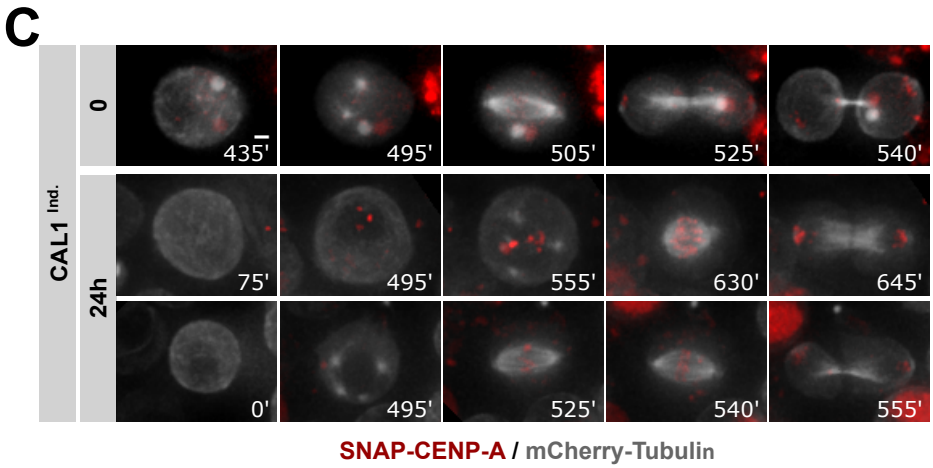

D

	Ctrl		CAL1 induction	
SNAP-CENP-A + cells	38 %	(167/452)	91 %	(371/458)
SNAP-CENP-A signal:				
Before Mitosis	0		31 %	(114/371)
During mitosis	91 %	(152/167)	18 %	(67/371)
After cytokinesis	9 %	(15/167)	51 %	(191/371)

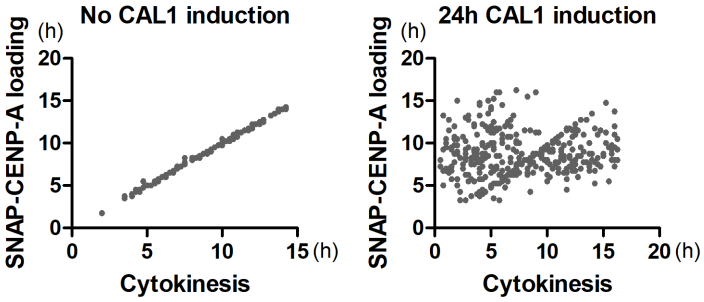

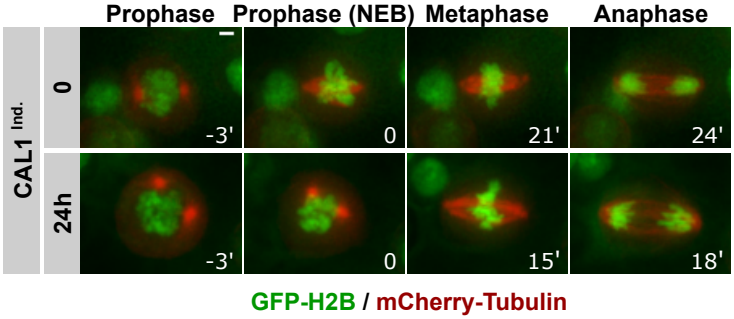

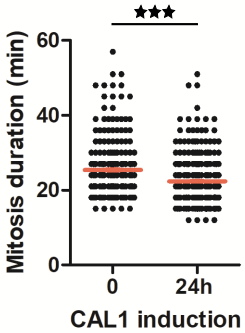

Fig.2

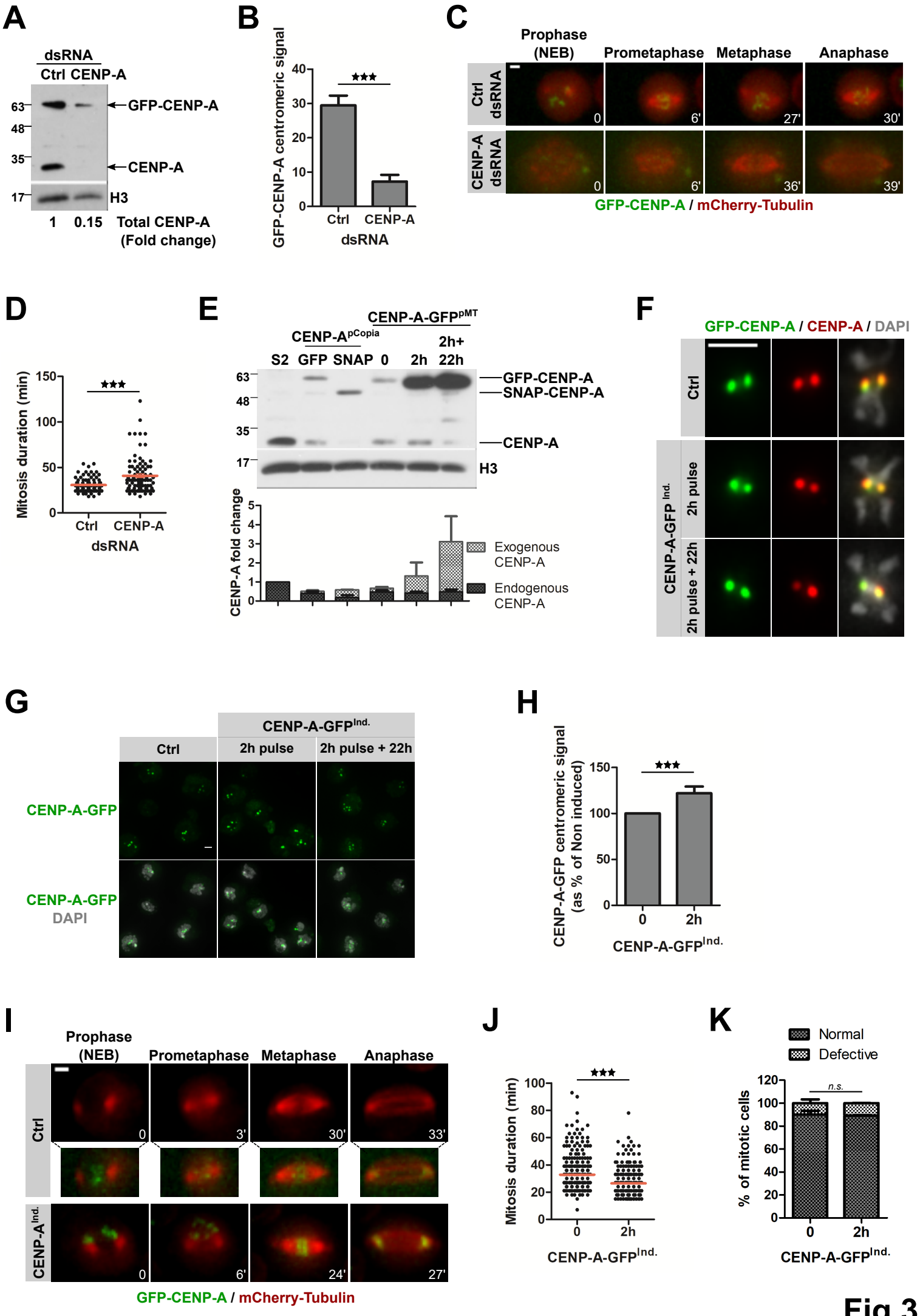
A
dsRNA
Ctrl CENP-A
63
48
35
17
GFP-CENP-A
CENP-A
H3
1 0.15 Total CENP-A (Fold change)
B
GFP-CENP-A centromeric signal
40
30
20
10
0
***
Ctrl CENP-A
dsRNA
C
Prophase (NEB)
Prometaphase
Metaphase
Anaphase
Ctrl dsRNA
CENP-A dsRNA
0
6'
27'
30'
0
6'
36'
39'
GFP-CENP-A / mCherry-Tubulin
D
Mitosis duration (min)
150
100
50
0
***
Ctrl CENP-A
dsRNA
E
CENP-A-GFP pMT
CENP-A pCopia
2h+
S2 GFP SNAP 0 2h 22h
63
48
35
17
GFP-CENP-A
SNAP-CENP-A
CENP-A
H3
CENP-A fold change
5
4
3
2
1
0
Exogenous CENP-A
Endogenous CENP-A
F
GFP-CENP-A / CENP-A / DAPI
Ctrl
CENP-A-GFP Ind.
2h pulse
2h pulse + 22h
G
CENP-A-GFP Ind.
Ctrl
2h pulse
2h pulse + 22h
CENP-A-GFP
CENP-A-GFP
DAPI
H
CENP-A-GFP centromeric signal (as % of Non induced)
150
100
50
0
***
0 2h
CENP-A-GFP Ind.
I
Prophase (NEB)
Prometaphase
Metaphase
Anaphase
Ctrl
0
3'
30'
33'
CENP-A Ind.
0
6'
24'
27'
GFP-CENP-A / mCherry-Tubulin
J
Mitosis duration (min)
100
80
60
40
20
0
***
0 2h
CENP-A-GFP Ind.
K
Normal
Defective
% of mitotic cells
120
100
80
60
40
20
0
n.s.
0 2h
CENP-A-GFP Ind.

Fig.3

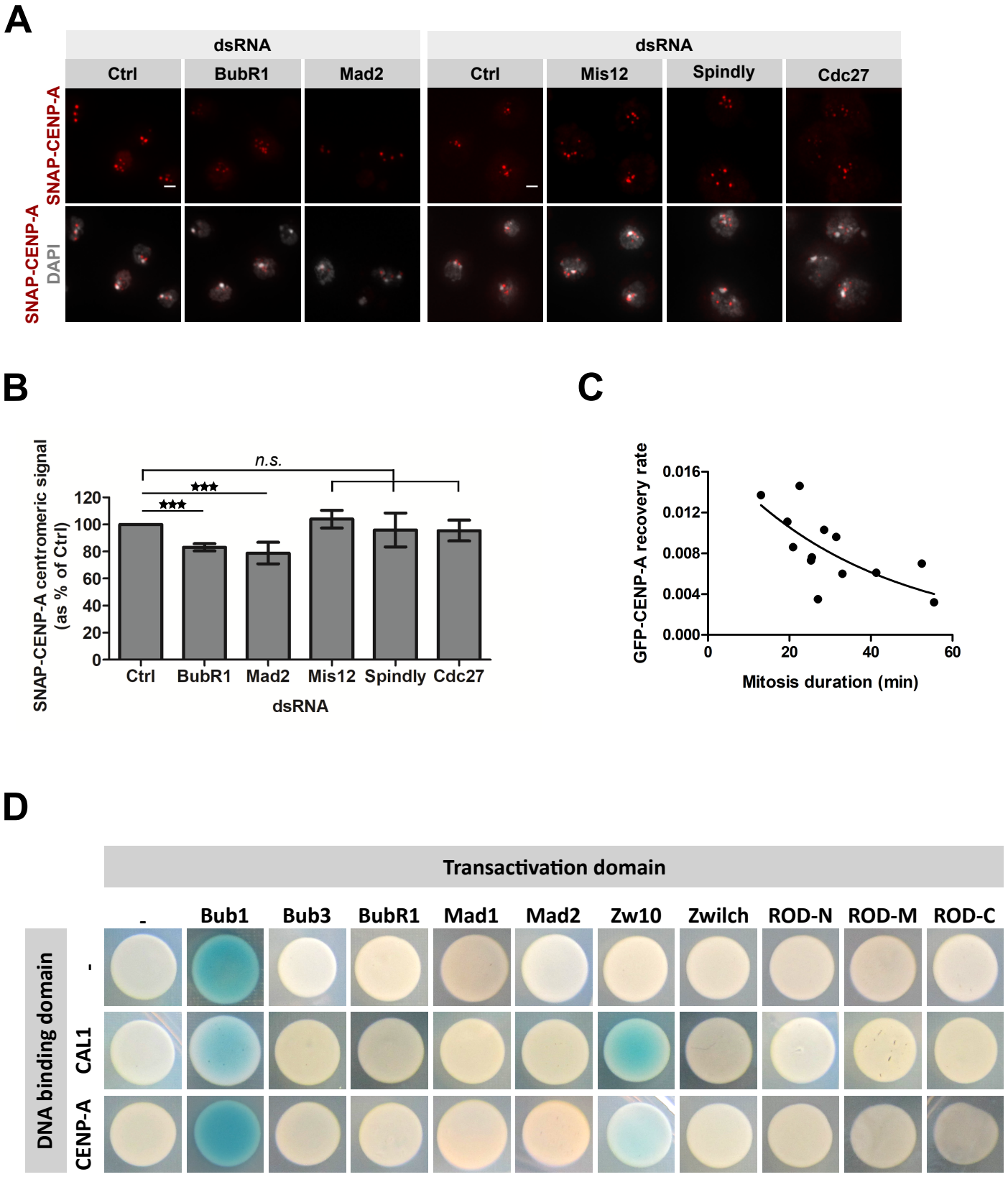
A
dsRNA
Ctrl
BubR1
Mad2
dsRNA
Ctrl
Mis12
Spindly
Cdc27
SNAP-CENP-A
SNAP-CENP-A
DAPI
B
SNAP-CENP-A centromeric signal (as % of Ctrl)
n.s.
***
***
120
100
80
60
40
20
0
Ctrl
BubR1
Mad2
Mis12
Spindly
Cdc27
dsRNA
C
GFP-CENP-A recovery rate
0.016
0.012
0.008
0.004
0.000
0
20
40
60
Mitosis duration (min)
D
Transactivation domain
-
Bub1
Bub3
BubR1
Mad1
Mad2
Zw10
Zwilch
ROD-N
ROD-M
ROD-C
DNA binding domain
-
CAL1
CENP-A

Fig.4

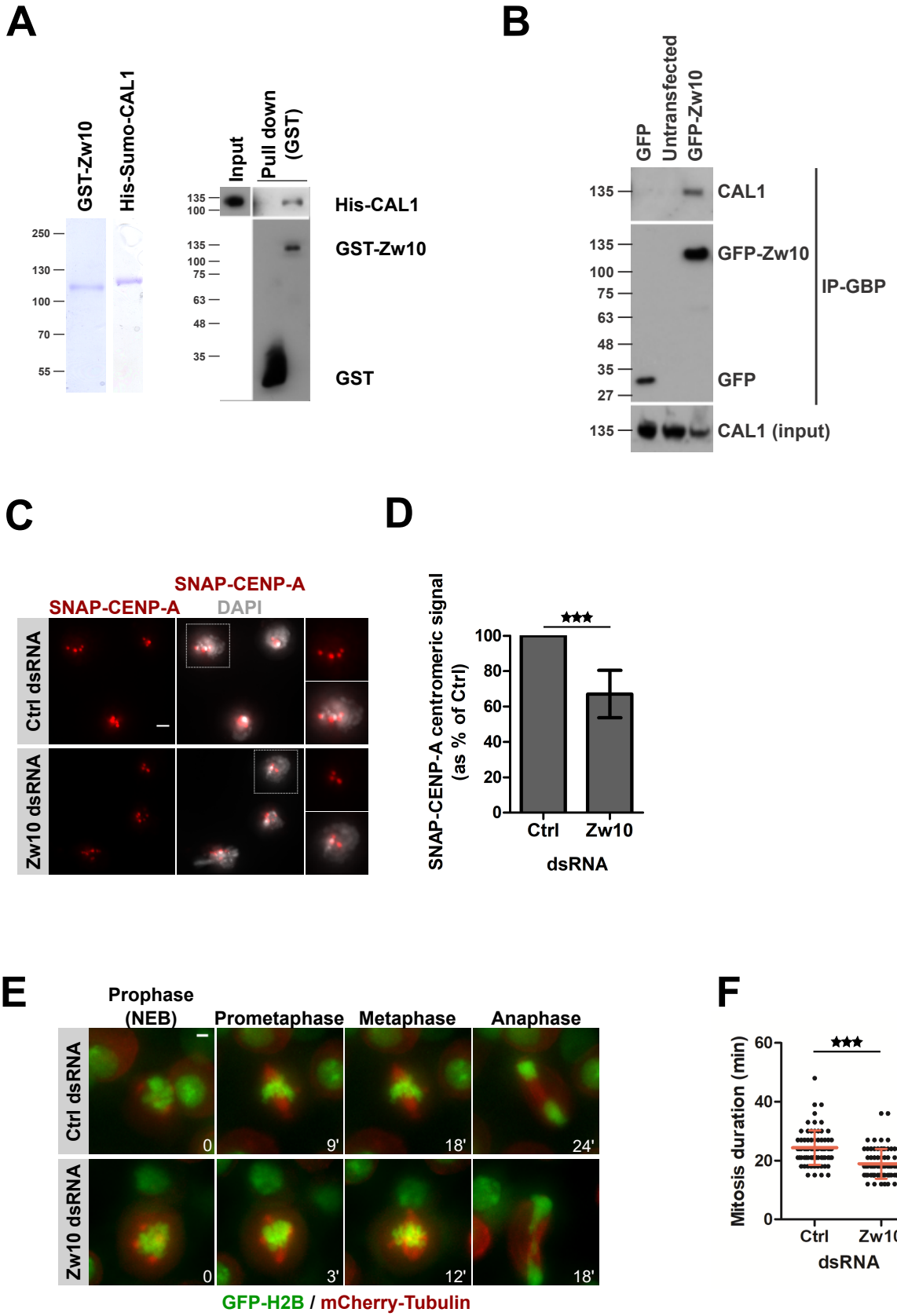
A
GST-Zw10
His-Sumo-CAL1
250
130
100
70
55
Input
Pull down (GST)
135
100
His-CAL1
135
100
75
63
48
35
GST-Zw10
GST
B
GFP
Untransfected
GFP-Zw10
135
CAL1
135
100
75
63
48
35
27
GFP-Zw10
GFP
IP-GBP
135
CAL1 (input)
C
SNAP-CENP-A
SNAP-CENP-A
DAPI
Ctrl dsRNA
Zw10 dsRNA
D
SNAP-CENP-A centromeric signal (as % of Ctrl)
100
80
60
40
20
0
***
Ctrl
Zw10
dsRNA
E
Prophase (NEB)
Prometaphase
Metaphase
Anaphase
Ctrl dsRNA
Zw10 dsRNA
0
9'
18'
24'
0
3'
12'
18'
GFP-H2B / mCherry-Tubulin
F
Mitosis duration (min)
60
40
20
0
***
Ctrl
Zw10
dsRNA

Fig.5

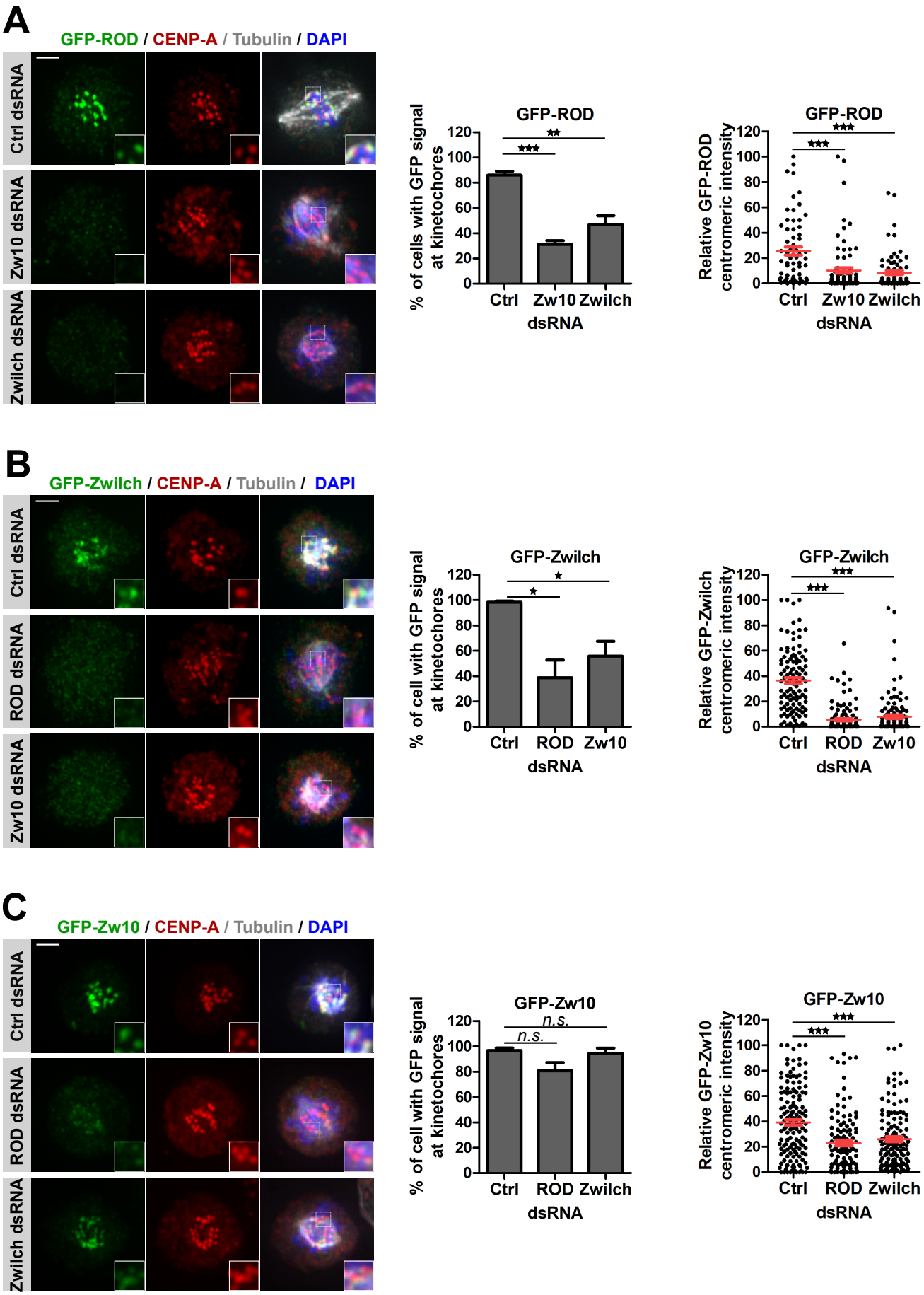
A
GFP-ROD / CENP-A / Tubulin / DAPI
Ctrl dsRNA
Zw10 dsRNA
Zwilch dsRNA
GFP-ROD
% of cells with GFP signal at kinetochores
Ctrl
Zw10
Zwilch
dsRNA
Relative GFP-ROD centromeric intensity
B
GFP-Zwilch / CENP-A / Tubulin / DAPI
Ctrl dsRNA
ROD dsRNA
Zw10 dsRNA
GFP-Zwilch
% of cell with GFP signal at kinetochores
Relative GFP-Zwilch centromeric intensity
C
GFP-Zw10 / CENP-A / Tubulin / DAPI
Ctrl dsRNA
ROD dsRNA
Zwilch dsRNA
GFP-Zw10
n.s.
Relative GFP-Zw10 centromeric intensity

Fig.6

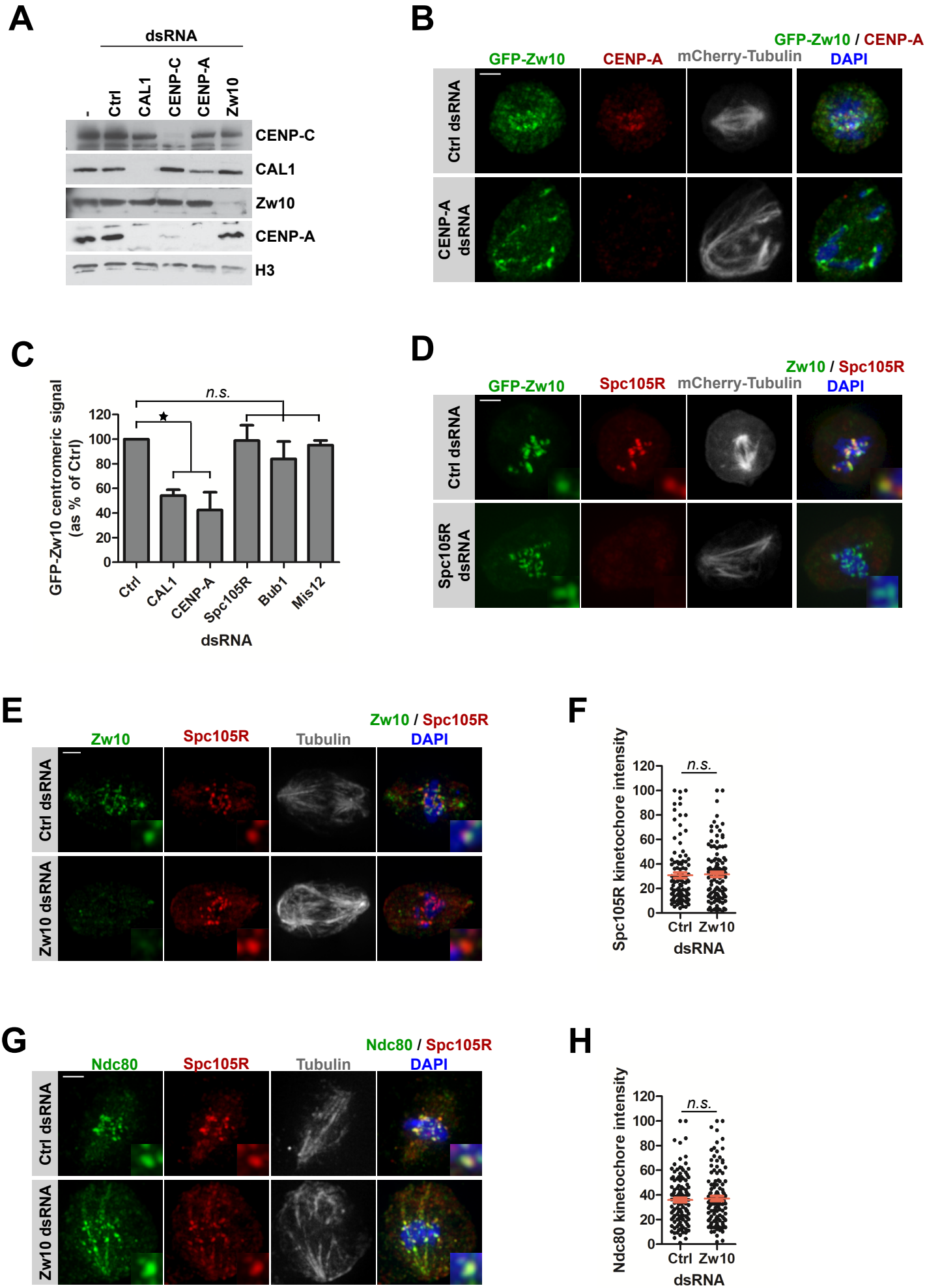
A
dsRNA
-
Ctrl
CAL1
CENP-C
CENP-A
Zw10
CENP-C
CAL1
Zw10
CENP-A
H3
B
GFP-Zw10 / CENP-A
GFP-Zw10
CENP-A
mCherry-Tubulin
DAPI
Ctrl dsRNA
CENP-A dsRNA
C
GFP-Zw10 centromeric signal (as % of Ctrl)
n.s.
120
100
80
60
40
20
0
Ctrl
CAL1
CENP-A
Spc105R
Bub1
Mis12
dsRNA
D
Zw10 / Spc105R
GFP-Zw10
Spc105R
mCherry-Tubulin
DAPI
Ctrl dsRNA
Spc105R dsRNA
E
Zw10 / Spc105R
Zw10
Spc105R
Tubulin
DAPI
Ctrl dsRNA
Zw10 dsRNA
F
Spc105R kinetochore intensity
n.s.
120
100
80
60
40
20
0
Ctrl
Zw10
dsRNA
G
Ndc80 / Spc105R
Ndc80
Spc105R
Tubulin
DAPI
Ctrl dsRNA
Zw10 dsRNA
H
Ndc80 kinetochore intensity
n.s.
120
100
80
60
40
20
0
Ctrl
Zw10
dsRNA

Fig.7